NRL REPORT NO. R-3167

TRANSFER CHARACTERISTICS OF A BRIDGED PARALLEL-T NETWORK

Charles F. White

Approved by:

Mr. P. Waterman, Head, Equipment Research Section
Dr. R. M. Page, Superintendent, Radio Division III

Program No. 36R05 August 27, 1947

NAVAL RESEARCH LABORATORY
COMMODORE H. A. SCHADE, USN, DIRECTOR
WASHINGTON, D.C.

DISTRIBUTION

GMC Committee, RDB, Wash., D. C.	A	(1)
CG, AAF, Wash., D. C., Attn: AC/AS-4, DRE-3, Pentagon	"	(2-5)
CG, AMC, Wright Field, Dayton, Ohio, Attn: TSEON-2	"	(6-30)
CG, Air Univ., Maxwell Field, Ala., Attn: Air Univ. Library	"	(31)
BuAer, Wash., D. C., Attn: TD-4	"	(32-37)
BuOrd, Wash., D. C., Attn: Re-9	"	(38-41)
BuShips, Wash., D. C., Attn: Codes 633, 910A, and 343	"	(42-44)
Ch/GMBranch, Technical Command, Army Chem. Center, Md.	"	(45)
CG, APG, Md., Attn: Ballistic Res. Lab.	"	(46)
CG, Eglin Field, Fla., Attn: First Exp., GM Group	"	(47)
CG, AAS, Fort Bliss, Texas	"	(48)
CO, Frankford Arsenal, Phila., Attn: Fire Control Design Div.	"	(49)
Commander, NAMC, Phila.	"	(50)
CO, NADS, Johnsville, Pa.	"	(51)
CO, ONR, San Francisco	"	(52-53)
CO, SCEL, Bradley Beach, N. J.	"	(54-55)
CO, NAMTC, Pt. Mugu, Calif.	"	(56)
CO, NOTS, Inyokern, Calif.	"	(57)
CO, Alamorgodo Army Air Base, N. M.	"	(58)
Dir., DTMB, Wash., 7, D. C., Attn: Aero. Mechanics Div.	"	(59)
Dir., NACA, Wash., D. C., Attn: Mr. C. H. Helms	"	(60-63)
Dir., NRL, Wash., 20, D. C.	"	(64-66)
Dir., Spec. Devices Center, ONR, Sands Point, L. I., Attn: TID	"	(67)
First Antiaircraft Artillery, GM Btn., White Sands Proving Ground	"	(68)
Head, PG School, U. S. Naval Academy, Annapolis	"	(69)
RDB, Attn: Library	"	(72)
Off. Ch/Ord, Res. and Dev. Div., Rocket Branch, Pentagon	"	(73)
OinC, BOEU, Hydraulics Bldg., Nat'l BuStds., Wash., D. C.	"	(74)
OinC, NOL, NavGun, Wash., D. C., Attn: Dr. R. J. Seeger	"	(75-76)
OinC, Ord. Res. and Dev. Div. Suboffice (Rocket) Ft. Bliss, Texas	"	(77)
CNO, Op-57	"	(78)
Watson Labs., AMC, Eatontown, N. J.	"	(79)
Watson Labs., AMC, Cambridge Field Station, Mass., Attn: Dr. M. O'Day	"	(80)
CG, Army Ground Forces, Ft. Monroe, Va., Attn: Ch/Dev. Sect. GNDEV-9	"	(81)
ONR, c/o Lib. of Congress, Tech. Info. Sect., Attn: J. Heald	"	(82-84)
Ch/Res. and Eng. Div., Off. Ch. Chem. Corps, Army Chem. Center, Md.	"	(85)
AEC, Div. Mil. Applic., Wash., 25, D. C., Attn: Col. D. J. Keirn	B	(1)
BAGR,-ED, NY Nav. Shipyard, Bldg. No. 3, Brooklyn 1, N. Y.	"	(2)
BAGR,-CD, Wright Field, Dayton, Ohio, Attn: Lt. Col. J. A. Gerath	"	(3)
BAGR,-WD, Los Angeles	"	(4)
BuOrd, Wash., 25, D. C., Attn: Re-9	"	(5-8)
CNO, Wash., 25, D. C., Attn: Op-34H, Op34H8, and Op-413	"	(9-11)
CG, AAF, Wash., 25, D. C., Attn: DC/AS, DRD	"	(13)
CG, APG, Md., Attn: Lib. Sect.	"	(15)
CG, AU, Maxwell Field, Attn: Lib. of AAFSSS, Craig Field, Ala.	"	(16)
CG, AU, Maxwell Field, Attn: Lib. for AAFTS, Tyndall Field, Fla.	"	(17)
Comdt., Command and Staff College, Ft. Leavenworth, Kansas	"	(18)
Comdt., Mar. Corps., Wash., D. C., Attn: G-3 (Special Weapons)	"	(19)
Comdt., Armed Forces Staff College, Norfolk 11, Va.	"	(20)
COM NATC, Patuxent River, Md., Attn: Dir. of Tests	"	(21)
CO, NAES, Phila., Attn: Supt. AEL	"	(22)
CO, NAOTS, Chincoteague, Va.	"	(23)
CO, Watertown Arsenal, Mass., Attn: Laboratory	"	(24)
ComOpDevFor, c/o Fleet Post Office, N. Y., N. Y.	"	(25-26)
Dir. Res. and Dev., War Dept. Gen Staff, Pentagon	"	(27)
Dir., Seacoast Service Test Sect. AFG Board No. 1, Ft. Baker, Calif.	"	(28)

Hd. Ord. and Gunnery, USNA, Annapolis	B	(29)
OCO, Ord. Res. and Dev. Serv., Ammunition Branch, Pentagon	"	(30)
OCSigO, Engr. and Tec. Serv., Engr. Div., Pentagon	"	(31)
Off. Sec. of War, Pentagon	"	(32)
Ord. Adv. Comm. on GM, General Radio Co., Cambridge 39, Attn: Dr. H. B. Richmond	"	(34)
Pres. Army Ground Forces Board No. 1, Ft. Bragg, N. C.	"	(35)
Pres. Army Ground Forces Board No. 4, Ft. Bliss, Texas	"	(36)
Prof. of Ord., U. S. Military Academy, West Point, N. Y.	"	(37)
Sec. Special Board, Comdt. of Marine Corps, Marine Corps School, Quantico	"	(38)
National War College, Wash., D. C.,Attn: Library	"	(39)
DCO for APL, JHU, Silver Spring, Md.	C	(1-3)
BAR, Buffalo, for BAC, Niagara Falls, Attn: Mr. R. H. Stanley and Mr. Hamlin	"	(4)
BTL, Murray Hill, N. J., Attn: W. A. MacNair	"	(5)
Bendix Av. Corp., East Teteboro, N. J., Attn: Dr. H. Selvidge	"	(6)
Boeing Aircraft Corp., Seattle, Attn: Mr. R. H. Nelson	"	(7)
DCO for C-V Air. Corp., LSL, Daingerfield, Texas, Attn: Mr. Arnold	"	(8)
BAR, Consolidated-Vultee Air. Corp., San Diego, Attn: Mr. Ables	"	(9)
DCO for Cornell Aero. Lab., Buffalo, N. Y., Attn: Mr. W. M. Duke	"	(10)
BAR for Curtiss-Wright Corp., Columbus, Attn: Mr. B. Eaton	"	(11)
BAR for Douglas Aircraft Co., El Segundo, Calif., Attn: Mr. Heinemann	"	(12)
Douglas Air. Co., Santa Monica, Attn: Mr. A. E. Raymond, (Project Rand) and Mr. E. F. Burton	"	(13-14)
INSORD for Eastman Kodak Co., Rochester, N. Y., Attn: Dr. Trotter	"	(15)
Fairchild Eng. and Air. Corp., NEPA Div., Oak Ridge, Attn: Mr. Kalitinsky	"	(16)
RIC-BuAer for Fairchild Eng. and Air. Corp., Farmingdale, Attn: J. A. Slonin	"	(17)
CO, NADS for Franklin Inst. Labs., Phila., Attn: Mr. R. H. McClarren	"	(18)
Gen. Elec. Co., Schenectady, Project HERMES, Attn: Mr. C. K. Bauer	"	(19)
DCO for G. E. Co., Schenectady, Attn: A. L. Ruiz	"	(20)
G. E. Co., Av. Div., Schenectady, Attn: Mr. S. A. Schuler, and Mr. P. Class	"	(21)
BAR for Glenn L. Martin Co., Balt., Attn: Mr. N. M. Voorhies	"	(22)
Glenn L. Martin, Balt., Attn: Mr. W. B. Bergen	"	(23)
INSMAT, Chicago for Globe Corp., Joliet, Ill., Attn: Mr. J. A. Weagle	"	(24)
BAR for Goodyear Aircraft Corp., Akron, Attn: Dr. Carl Arnstein	"	(25)
Goodyear Aircraft, Plant B, Akron, Attn: Mr. A. J. Peterson	"	(26)
BAR for Grumman Air. Engr. Corp., Bethpage, L. I., Attn: Mr. Schwendler	"	(27)
Hughes Aircraft Co., Culver City, Calif., Attn: Mr. D. H. Evans	"	(28)
OinC, Res. and Dev. Serv. Suboffice (Rocket) CIT, Pasadena	"	(29-30)
INSMAT for Kellex Corp., New York, N. Y.	"	(31)
M. W. Kellogg Co., Jersey City, N. J., Attn: Dr. G. H. Messerly	"	(32)
NORTLO for Chairman, MIT, GMC, Project Meteor Office, Cambridge, Attn: Dr. H. G. Stever	"	(33-34)
BAR for McDonnell Aircraft Corp., St. Louis, Attn: W. P. Montgomery	"	(35)
BAR for NAA, Inc., Los Angeles, Attn: Mr. D. H. Mason	"	(36)
Northrop Aircraft Inc., Hawthorne, Calif.	"	(37)
DCO for P. U. Phys. Dept., Princeton, N. J., Attn: Mr. Harry Ashworth	"	(38)
CO, ONR Branch Office, N. Y. for Princeton U., Attn: Proj. SQUID	"	(39-41)
INSMAT for Radio Corp. of America, Camden, N. J.,Attn: Mr. T. T. Eaton	"	(42)
BAR for Radioplane Corp, Van Nuys, Calif., Attn: Mr. Ferris Smith	"	(43)
INSMAT, Boston, for Raytheon Mfgr. Co., Waltham, Attn: Mrs. H. L. Thomas	"	(44)
INSMAT, Brooklyn, for Reeves Instrument Corp., N. Y., N. Y.	"	(45)
Republic Aviation Corp., Farmingdale, L. I., Attn: Dr. Wm. O'Donnell	"	(46)
Ryan Aero. Co., Lindberg Field, San Diego 12, Calif., Attn: Mr. H. A. Sutton	"	(47)
INSMAT, Brooklyn, for Sperry Gyroscope Co, Great Neck, L. I.	"	(49)
BAR, U. A. Corp., Stratford, for U. A. Corp, Chance Vought Air. Div., Stratford, Conn.,Attn: Mr. P. S. Baker	"	(50)
BAR, U. A. Corp., E. Hartford, for U. A. Corp., Research Dept., E. Hartford, Attn: Mr. J. G. Lee	"	(51)
Univ. of Mich., Aero. Res. Center, Willow Run Airport, Attn: R. F. May and Dr. A. M. Kuethe	"	(52)
BAR, Pasadena for USC, Naval Res. Proj., LA, Attn: Dr. R. T. DeVault	"	(53)
DCO, Univ. of Texas, Defense Res. Lab., Austin, Attn: Dr. C. P. Boner	"	(54)
Lockheed Aircraft Corp., Burbank, Calif., Attn: Mr. H. L. Hibbard	"	(56)
Calif. Inst. of Tech., JPL, Pasadena, Attn: Mr. L. G. Dunn	"	(57)

CONTENTS

ABSTRACT

The parallel-T resistance-capacitance null-type network together with a bridging and a re-tuning resistance when operated between suitably selected generator and load resistances exhibits a wide range of response characteristics. General formulas for the steady-state response of the network are derived and the effects of variation of the parameters relating to network symmetry, bridging resistance, generator resistance, and load resistance are shown by means of families of curves that serve as useful design data in the wide range of applications to which the parallel-T network may be applied. Used for frequency response control in servo systems employing amplitude-modulated carrier voltages for data transmission, the network provides carrier suppression and symmetrical sideband transmission of controllable characteristics with resulting system simplification.

PROBLEM STATUS

This report represents completion of a study under the general long-term program No. R05.

TRANSFER CHARACTERISTICS OF A BRIDGED PARALLEL-T NETWORK

INTRODUCTION

The bridged paralled-T network consists of a basic parallel-T resistance-capacitance three-terminal network of unsymmetrical design to which has been added a bridging resistance placed across the upper input and output terminals together with a re-tuning resistance placed between the lower network terminal and the terminal common to both the input and the output circuits. The effects of the generator and load resistance are considered and are utilized to obtain additional variation in the frequency response of the circuit.

The analysis proceeds from a study of the basic unsymmetrical parallel-T network to a determination of the re-tuning resistance value required to prevent a shift in the frequency of maximum attenuation when the bridging resistance is in place and, finally, to a general equation for the frequency response of the complete circuit including the effects of generator and load resistance. In determining the effects of the four circuit parameters, namely, symmetry parameter, bridging-resistance parameter, generator-resistance parameter, and load-resistance parameter, particular cases of the general equation are derived for extreme or special values of the parameters not under study. The effects of each parameter are shown by means of families of curves that are supplemented by other special curves that add to the design data made available.

Of the wide range of possible frequency response characteristics shown, particular attention is given to the determination of the bridged-network design requirements for equal upper and lower side-band transmission for use in the frequency-response control of servo systems utilizing amplitude-modulated carrier voltages for data transmission. In such servo systems, it is not uncommon practice to obtain the error signal independent of the carrier by demodulation, then to insert frequency response controlling networks of conventional design, and finally to re-introduce the carrier by means of a similar circuit used as a modulator. Substantial system simplification results when the above circuits are replaced by the bridged parallel-T network.

HISTORICAL BACKGROUND

The parallel-T resistance-reactance filter resulted from an investigation by Augustadt[1]* of means for a more economical rectifier filter. A brief sketch of the steps taken in the

---

* Text superscripts refer to numbered references.

evolution of the network is of historical interest as an example of the results obtainable by properly directed analytical methods. From the basic structure of Figure 1, the symmetrical lattice equivalent shown in Figure 2 was formed and used in the analysis as the prototype structure. A peak of attenuation was obtained by M—deriving (Figure 3).

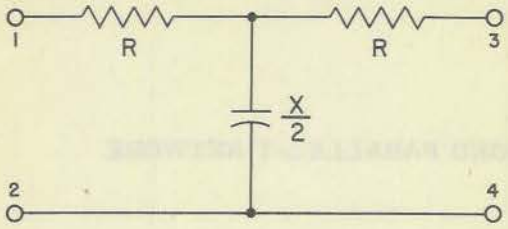

Fig. 1 - Basic Structure

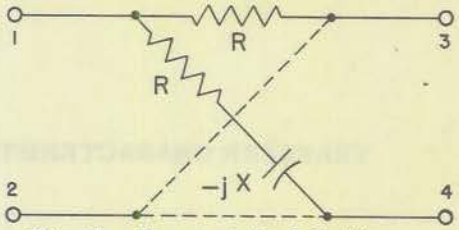

Fig. 2 - Symmetrical Lattice Equivalent of Basic Structure

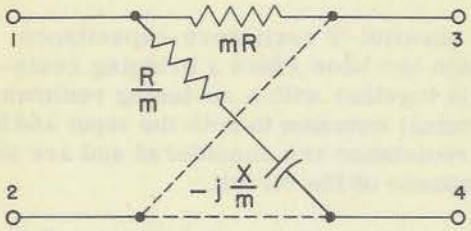

Fig. 3 - M-Derived Equivalent

From a study of the performance of the structure of Figure 3 it was found that for the peak of attenuation to occur at a real frequency, the prototype structure of Figure 2 must be M—derived with a complex "M"(Figure 4). Figure 5 is the lattice equivalent of Figure 4. A final transformation from the lattice structure to the more economical design of the parallel-T structure of Figure 6, in which the resistances R_1 may be lumped with the generator and load resistances, completed the evolution to the three-terminal network subsequently to become known as the parallel-T filter.

While the circuit of Figure 6 shows a pair of symmetrical T-networks, the patent[1] issued to Augustadt covers unsymmetrical designs and includes a correlation with the generator and load resistance effects on the circuit operation.

References 1-16 listed in this report cover other work previously done on this network and also indicate the importance of the network. The unsymmetrical design variation in the network was investigated by McGaughan[12] and is the design incorporated into the bridged parallel-T theory reported here.

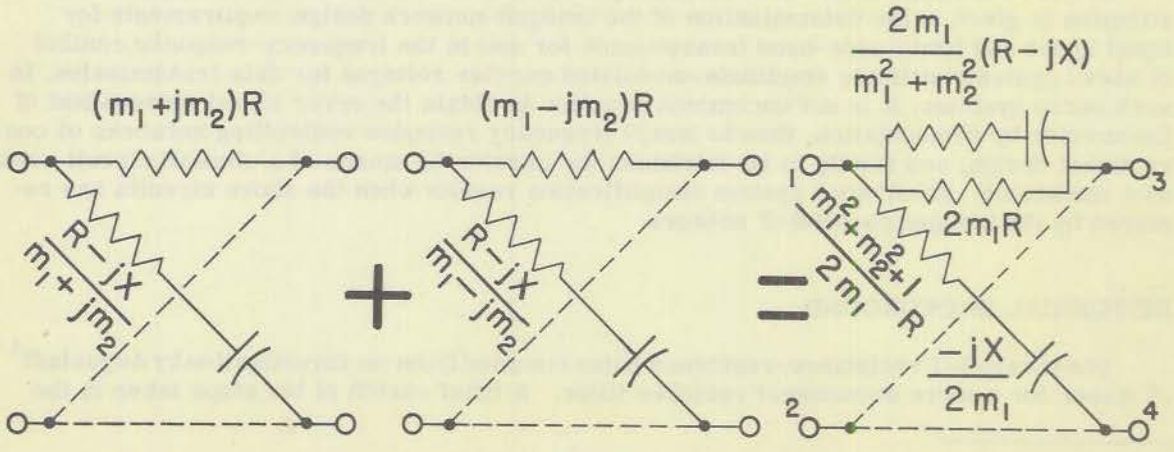

Fig. 4 - Complex M-Derived Configuration

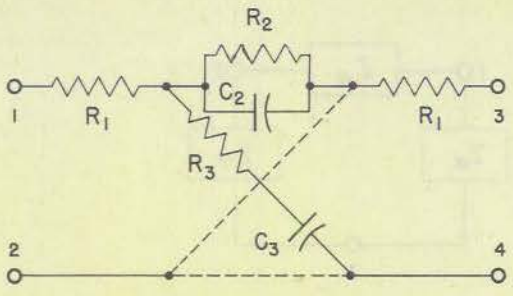

Fig. 5 - Lattice Equivalent of Fig. 4

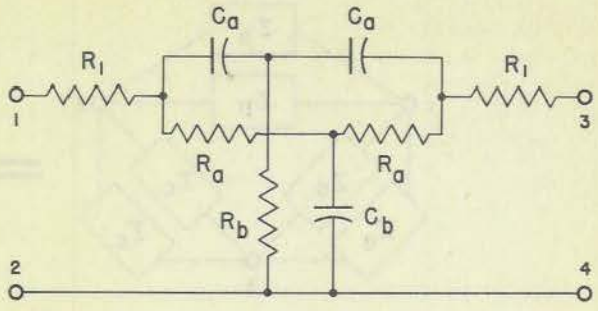

Fig. 6 - Parallel-T Equivalent of Fig. 5

BASIC NETWORK

The circuit configuration taken as the core of the bridged parallel-T network is a special case of that of Figure 7. The n and m are parameters that may be given any positive real values. Note that the time constant at each of the three terminals of the network equals R·C. As only circuits producing a true null are desired, a limitation must be placed on the values that n may assume. To obtain such a formula for n in terms of m, first consider the two T's separately and find their π-equivalents (Figures 8 and 9).

The combination of the two networks in parallel is shown by Figure 10 in which a single π-equivalent is indicated.

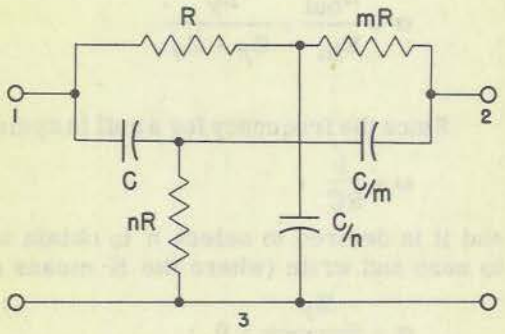

Fig. 7 - Unsymmetrical Parallel-T Configuration

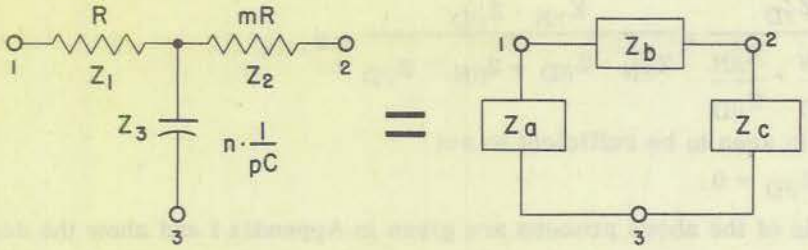

Fig. 8 - T-to-π Transformation of T Involving Two Resistances

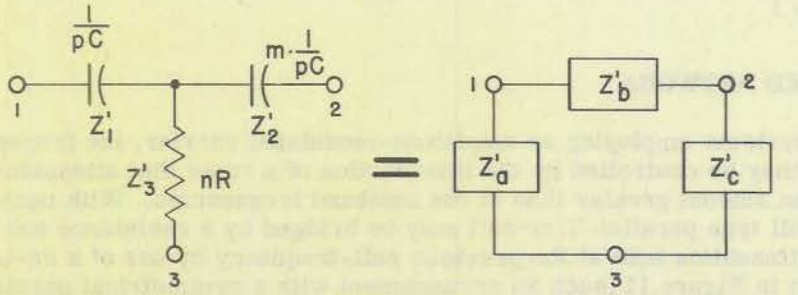

Fig. 9 - T-to-π Transformation of T Involving Two Capacitances

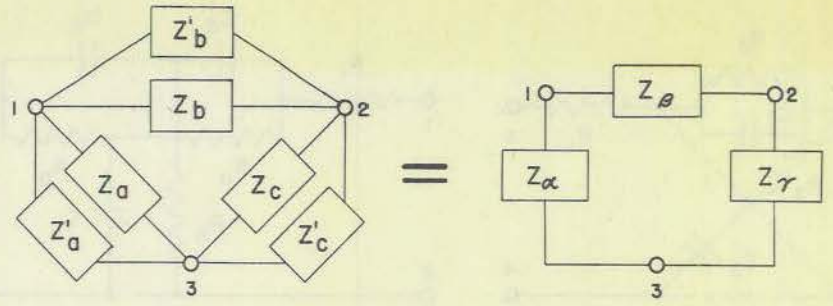

Fig. 10 - Parallel-π to Equivalent-π

The transfer characteristic, α, of the network in the absence of generator or load resistance is identically equal to

$$\alpha = \frac{E_{out}}{E_{in}} = \frac{Z_\gamma}{Z_\beta + Z_\gamma} \tag{1}$$

Since the frequency for a null in symmetrical parallel-T networks is known[1] and equals

$$\omega = \frac{1}{RC}\,, \tag{2}$$

and it is desired to select n to obtain a null at the same frequency, we may set α equal to zero and write (where the N means numerator and the D means denominator)

$$\alpha = \frac{Z_\gamma}{Z_\gamma + Z_\beta} = 0\,,$$

$$\alpha = \frac{\dfrac{Z_{\gamma N}}{Z_{\gamma D}}}{\dfrac{Z_{\gamma N}}{Z_{\gamma D}} + \dfrac{Z_{\beta N}}{Z_{\beta D}}} = \frac{Z_{\gamma N} \cdot Z_{\beta D}}{Z_{\gamma N} \cdot Z_{\beta D} + Z_{\beta N} \cdot Z_{\gamma D}} = 0\,, \tag{3}$$

from which it is seen to be sufficient to set

$$Z_{\gamma N} \cdot Z_{\beta D} = 0\,. \tag{4}$$

The details of the above process are given in Appendix I and show the desired relationship to be

$$n = \frac{m}{m+1}\,. \tag{5}$$

BASIC BRIDGED NETWORK

In servo systems employing an amplitude-modulated carrier, the frequency response of the system may be controlled by the introduction of a filter that attenuates at the carrier frequency by an amount greater than at the sideband frequencies. With such an application in mind, the null type parallel-T circuit may be bridged by a resistance and the frequency of maximum attenuation held at the previous null-frequency by use of a re-tuning resistance as shown in Figure 11 (such an arrangement with a symmetrical parallel-T network, m = 1, was used in certain radar equipment during the war).

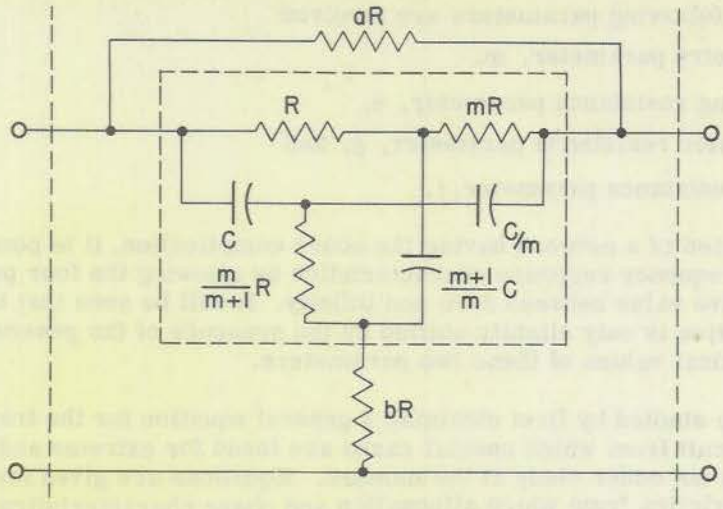

Fig. 11 - Bridged Parallel-T Configuration

At this point, it must be established that it is possible to accomplish the results desired, and a relationship must be found for the re-tuning resistance parameter, b, in terms of the symmetry parameter, m, and the bridging resistance parameter, a. These details are given in Appendix II and the resulting relationship is found to be

$$b = \frac{m}{2a}. \qquad (6)$$

THE BRIDGED PARALLEL-T NETWORK WITH GENERATOR AND LOAD RESISTANCE CONSIDERED

The foregoing material has led to the circuit that is the subject of the present report. Figure 12 shows a network consisting of a null-type unsymmetrical parallel-T resistance-capacitance structure with a bridging resistance and a re-tuning resistance, operated between a generator having resistance and a resistance load.

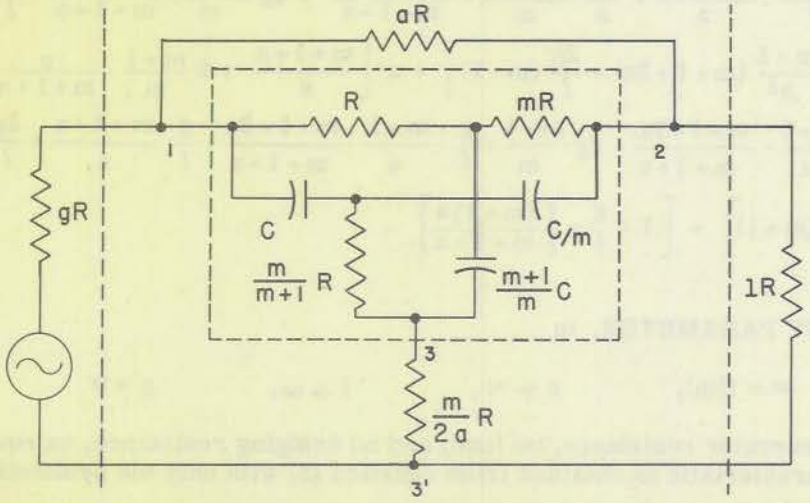

Fig. 12 - The Bridged Parallel-T Network

Note that the following parameters are involved:

(1) symmetry parameter, m,

(2) bridging resistance parameter, a,

(3) generator resistance parameter, g, and

(4) load resistance parameter, l.

As could be expected of a network having the above complication, it is possible to obtain a wide range of frequency response characteristics by allowing the four parameters to assume any positive value between zero and infinity. It will be seen that the frequency of maximum attenuation is only slightly shifted by the presence of the generator and load resistance for practical values of these two parameters.

The circuit is studied by first obtaining a general equation for the transfer characteristic of the circuit from which special cases are found for extreme and special values of the parameters not under study at the moment. Equations are given for the complex transfer characteristics from which attenuation and phase characteristics may be found. The details of the derivation of the general equation are given in Appendix III. The transfer characteristic is given as the ratio of the voltage, E_{out}, appearing across the load resistance to the open-circuit voltage, E_{in}, of the generator and is indicated by the symbol α. In the equation, the variable

$$u = pCR = \frac{p}{1/CR} = \frac{p}{\omega_0} = j\frac{\omega}{\omega_0} \tag{7}$$

where $\omega = 2\pi f$ and f = frequency in cycles per second. The equation is

$$\alpha = \left[u^2 + u\,\frac{m+1}{a}\cdot\frac{m+1+2a}{m+1+a} + 1\right]\left[1 + u\,\frac{m+1+a}{a}\right]\Big/\Delta \tag{8}$$

where $\Delta = u^3\left[\frac{m+1+a}{a} + 2g\,\frac{m+1}{m} + \frac{g}{l}\frac{m+1+a}{a}\right] + u^2\left[1 + 2\,\frac{m+1}{m} + \frac{m+1}{a^2}\,(m+1+2a)\right.$

$$+\frac{m+1}{l}\cdot\frac{m+1+a}{a} + \frac{2g}{a}\cdot\frac{(m+1)^2}{m}\cdot\frac{m+1+2a}{m+1+a} + 4g\,\frac{m+1}{m}\cdot\frac{a}{m+1+a} + \frac{g}{l}$$

$$\left.+\frac{g}{l}\frac{m+1}{a^2}\,(m+1+2a) + \frac{2g}{l}\,(m+1)\right] + u\left[\frac{m+1+a}{a} + 2\,\frac{m+1}{m}\cdot\frac{a}{m+1+a}\right.$$

$$+\frac{m+1}{a}\cdot\frac{m+1+2a}{m+1+a} + 2g\,\frac{m+1}{m} + \frac{g}{l}\cdot\frac{m+1}{a}\cdot\frac{m+1+2a}{m+1+a} + \frac{g}{l}\,\frac{m+1+a}{a} + \frac{2g}{l}\,\frac{(m+1)a}{m+1+a}$$

$$\left.+\frac{2}{l}(m+1)\right] + \left[1 + \frac{g}{l} + \frac{1}{l}\,\frac{(m+1)a}{m+1+a}\right] .$$

THE SYMMETRY PARAMETER, m

$$\alpha = f(m), \qquad a \to \infty, \qquad l \to \infty, \qquad g = 0$$

For zero generator resistance, no load, and no bridging resistance, an equation for the transfer characteristic is obtained from equation (8) with only the symmetry parameter, m, present.

Thus, $$\alpha = \frac{(u^2+1)(u+1)}{u^3 + u^2\left[1+2+\frac{2}{m}\right] + u\left[1+2+\frac{2}{m}\right] + 1}$$

$$= \frac{(u^2+1)}{u^2 + u\left[2+\frac{2}{m}\right] + 1} \quad . \tag{9}$$

Replacing the variable u by p/ω_o and factoring,

$$\alpha = \frac{\left[1+\frac{\omega}{\omega_o}\right]\left[1-\frac{\omega}{\omega_o}\right]}{\left[1+\frac{p}{\omega_o}\left[1+\frac{1}{m}+\sqrt{\frac{2}{m}+\frac{1}{m^2}}\right]\right]\left[1+\frac{p}{\omega_o}\left[1+\frac{1}{m}-\sqrt{\frac{2}{m}+\frac{1}{m^2}}\right]\right]} \tag{10}$$

where $\omega_o = \frac{1}{RC}$ and $p = j\omega$ as previously indicated.

The expression for α was put into the form shown in equation (10) to show clearly the effect of variation of the symmetry parameter. The two numerator factors are not influenced but the location of the two "low-pass corners" of the denominator are shifted to cause the variation in the attenuation and phase-shift characteristics of the network. Figure 13 shows the attenuation due to each of four factors of equation (10) evaluated for m = 1 together with the combined effect of these factors. The corresponding phase shift is shown by Figure 14.

Note that for variation of the value of m, the shape of the individual curves is not changed; only the position on the frequency axis is shifted. Table 1* gives the attenuation and phase shift associated with each of the terms $(1+\omega/\omega_o)$, $(1-\omega/\omega_o)$, and $1/(1+p/\omega_o)$ as used in preparing the curves. The first two factors are either positive or negative real quantities but the third is complex and it becomes necessary to calculate magnitude and phase.

The family of curves in Figure 15 shows the sharper attenuation characteristics obtainable with increasing values of m. It is possible to realize experimentally satisfactory networks with a value of m = 10. Note that for m = 10 almost all the possible improvement is obtained. Table 2 represents the data used in plotting the curves of Figure 15. That a complete null occurs at the frequency $\omega = \omega_o$ is made more evident by Figure 16 which is a percentage-transmission plot rather than decibels-attenuation plot of the same family of curves. Figure 17 has been prepared as an aid in selecting the value of m for a particular frequency bandwidth (as evaluated at the -3 db level) expressed in decades (a ten-to-one frequency range).

THE GENERATOR RESISTANCE PARAMETER, g

$$\alpha = f(g), \qquad a \to \infty, \qquad l \to \infty, \qquad m = 1$$

For a symmetrical parallel-T network, unbridged and with no load, an equation for the transfer characteristic involving the generator resistance parameter, g, is obtained from equation (8) and is

$$\alpha = \frac{(u^2+1)(u+1)}{u^3(1+4g) + u^2(5+8g) + u(5+4g) + 1}$$

$$= \frac{u^2+1}{u^2(1+4g) + u(4+4g) + 1} \quad . \tag{11}$$

* All tables are located in Appendix V.

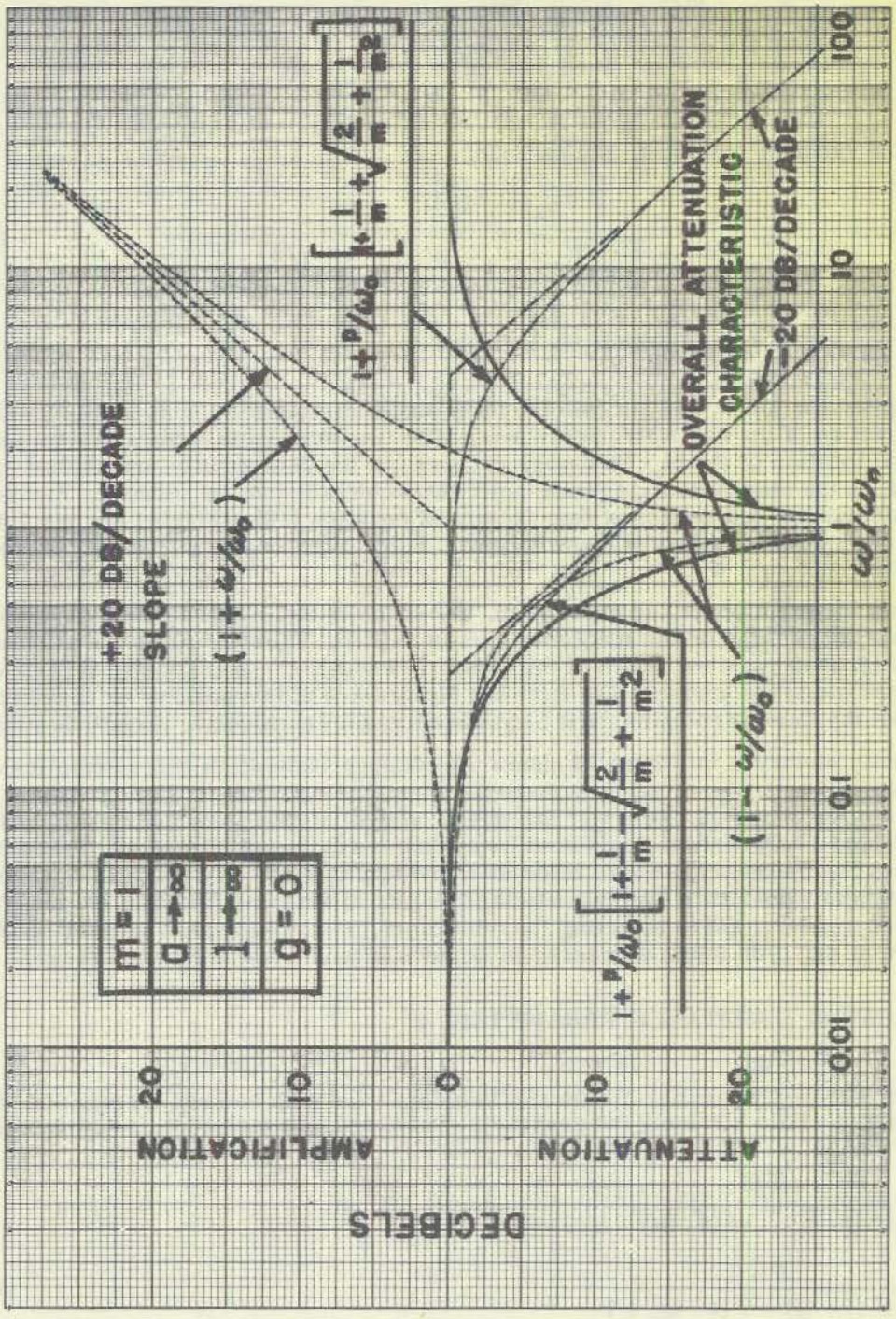

Fig. 13 - Attenuation Characteristics

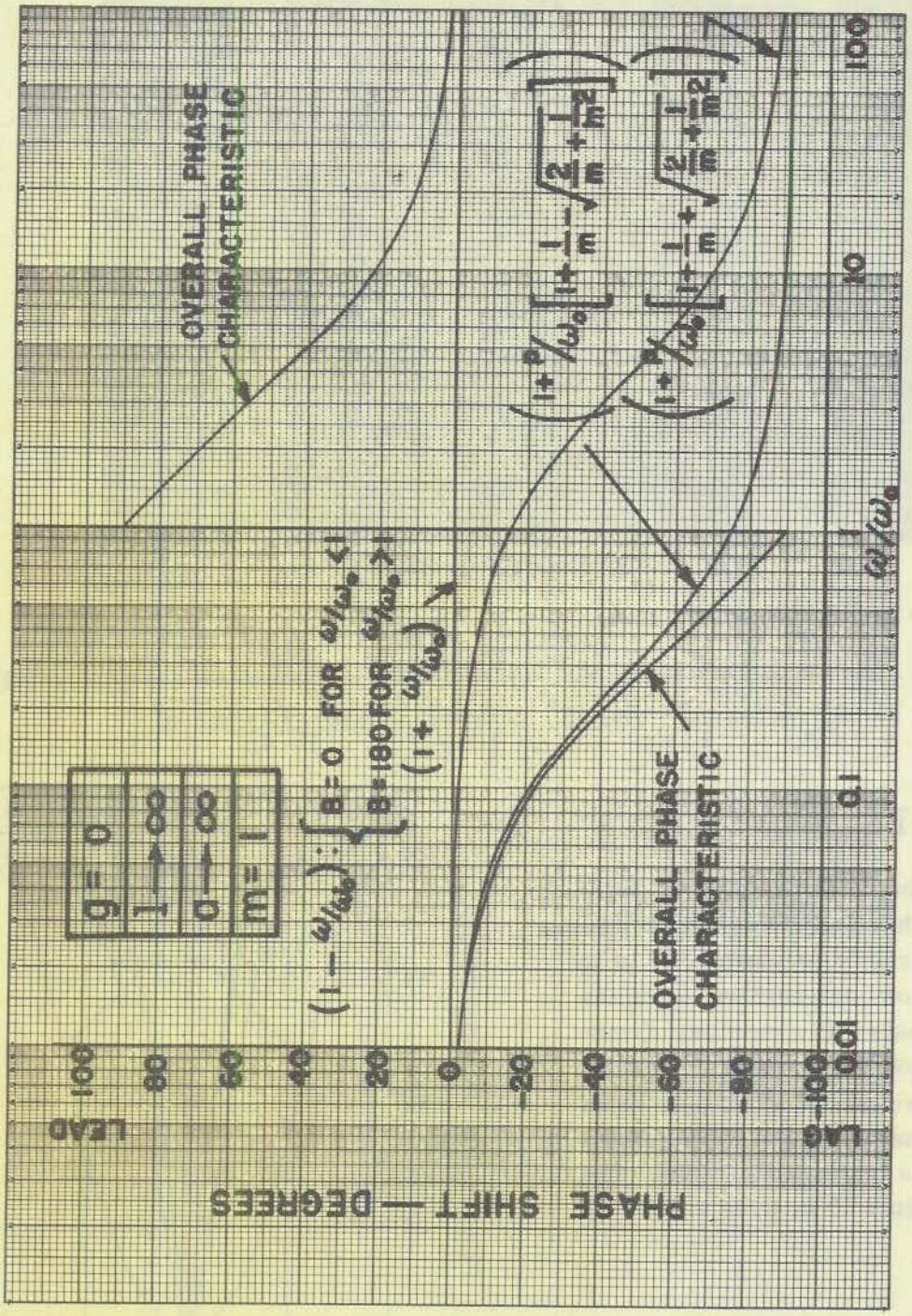

Fig. 14 - Phase Characteristics

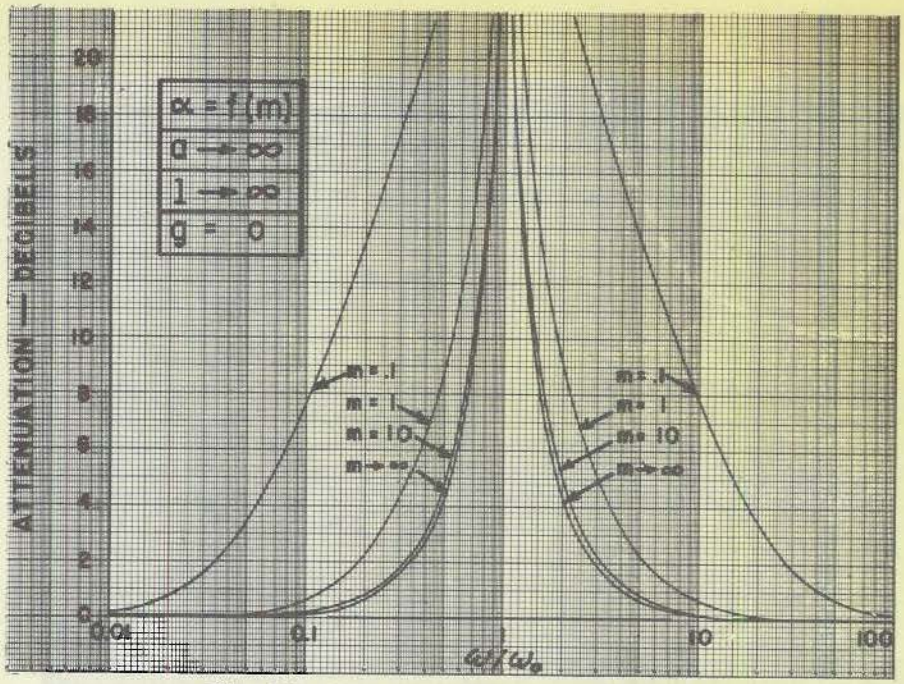

Fig. 15 - Symmetry Parameter Effects

Replacing u by $\frac{p}{\omega_o}$ and factoring,

$$\alpha = \frac{\left[1 + \frac{\omega}{\omega_o}\right]\left[1 - \frac{\omega}{\omega_o}\right]}{\left[1 + p/\omega_o\left[\frac{2 + 2g + \sqrt{3 + 4g + 4g^2}}{1 + 4g}\right]\right]\left[1 + p/\omega_o\left[\frac{2 + 2g - \sqrt{3 + 4g + 4g^2}}{1 + 4g}\right]\right]} \qquad (12)$$

where $\omega_o = \frac{1}{RC}$ and $p \equiv j\omega$.

As in the case of varying the parameter m, the effect of varying the generator resistance parameter, g, is to move the "low-pass corners" along the frequency axis with a resulting change in attenuation as shown by Figure 18. The most pronounced effect to be noted is an increase in the loss at high frequencies as g is increased in value. The data for Figure 18 is given in Table 3.

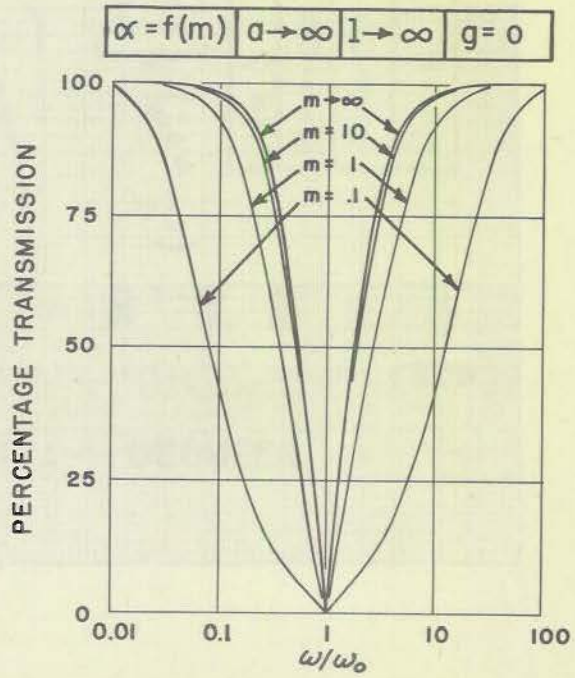

Fig. 16 - Percentage Transmission Curves

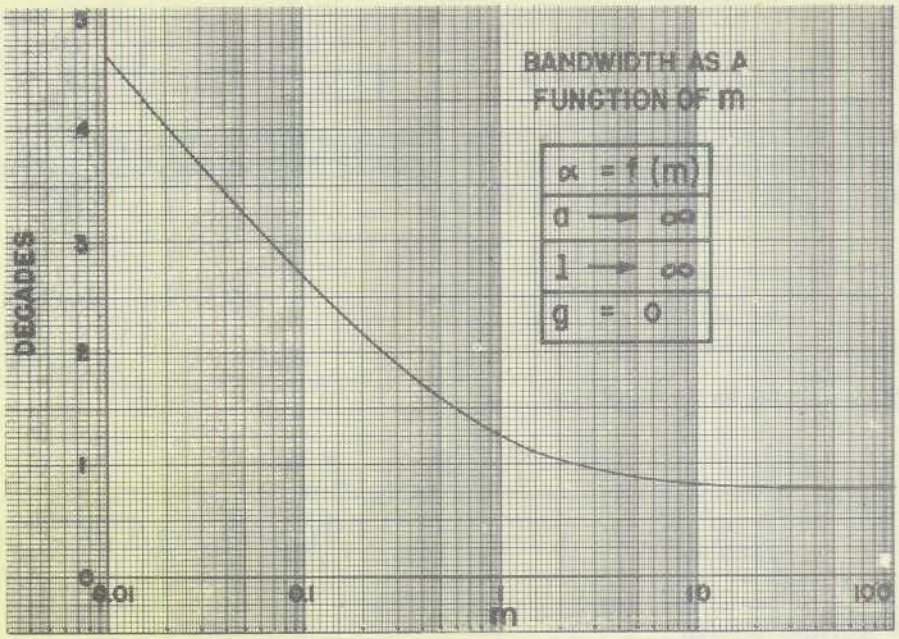

Fig. 17 - Bandwidth vs Symmetry Parameter

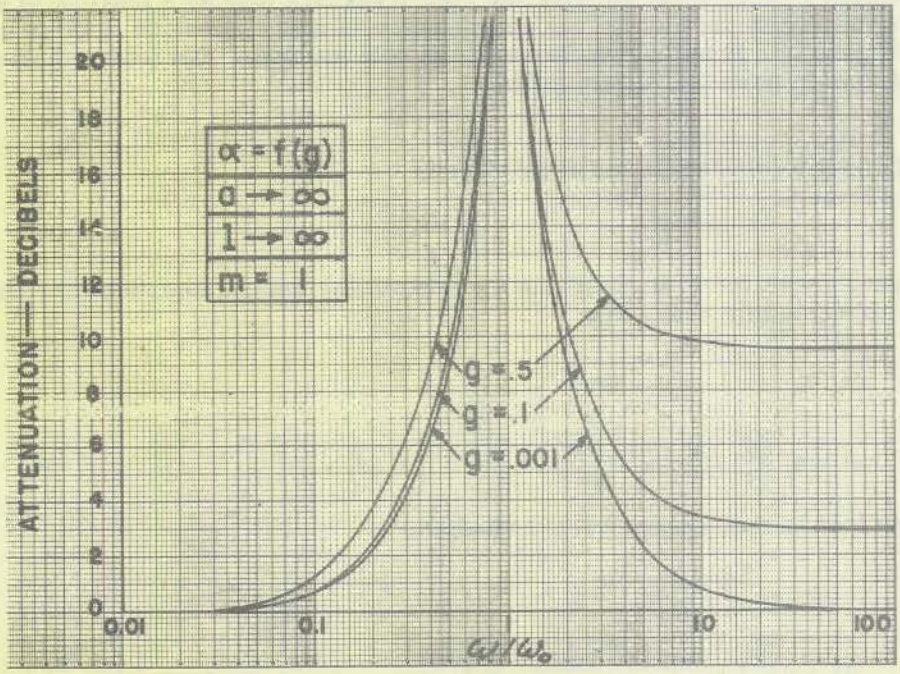

Fig. 18 - Generator Resistance Effects

THE LOAD RESISTANCE PARAMETER, l

$$\alpha = f(l), \qquad a \to \infty, \qquad g = 0, \qquad m = 1$$

For a symmetrical parallel-T network, unbridged and with zero generator resistance, the equation for the transfer characteristic involving the load resistance parameter l, obtained as a special case of equation (8), is

$$\alpha = \left[\frac{l}{l+2}\right] \frac{u^2 + 1}{u^2\left[\frac{l}{l+2}\right] + u\left[\frac{4l+2}{l+2}\right] + 1} \quad . \tag{13}$$

Replace u by $\frac{p}{\omega_o}$ and factor to obtain

$$\alpha = \left[\frac{l}{2+l}\right] \frac{\left[1 + \frac{\omega}{\omega_c}\right]\left[1 - \frac{\omega}{\omega_o}\right]}{\left[1 + p/\omega_o\left[2 + \frac{1}{l} - \sqrt{3 + \frac{2}{l} + \frac{1}{l^2}}\right]\right]\left[1 + p/\omega_o\left[2 + \frac{1}{l} + \sqrt{3 + \frac{2}{l} + \frac{1}{l^2}}\right]\right]} \tag{14}$$

where $\omega_o = \frac{1}{RC}$ and $p \equiv j\omega$.

The effect of variation of the parameter l is shown by Figure 19 in which it is noted that the loss at low frequencies increases with decrease in the value of l but that other portions of the attenuation characteristic are only slightly influenced. The data for Figure 19 is given in Table 4.

An auxiliary curve sheet showing the high-frequency loss as a function of generator resistance and the low-frequency loss as a function of load resistance is given as a design aid. See Figure 20. Simultaneous presence of both generator and load resistance results in some deviation from the values shown.

THE BRIDGING RESISTANCE PARAMETER, a

$$\alpha = f(l, a), \qquad g = 0, \qquad m = 1$$

For zero generator resistance and a symmetrical design, equation (8) reduces to the transfer characteristic defined by

$$\alpha = \frac{u^2 + u\left[\frac{4}{a} \cdot \frac{a+1}{a+2}\right] + 1}{u^2 + u\left[\frac{4}{a} \cdot \frac{a+1}{a+2} + \frac{4a}{a+2} + \frac{2}{l}\right] + \left[1 + \frac{2}{l} \cdot \frac{a}{a+2}\right]} . \tag{15}$$

For no load ($l \to \infty$), equation (15) reduces to

$$\alpha = \frac{u^2 + u\left[\frac{4}{a} \cdot \frac{a+1}{a+2}\right] + 1}{u^2 + u\left[\frac{4}{a} \cdot \frac{a+1}{a+2} + \frac{4a}{a+2}\right] + 1} . \tag{16}$$

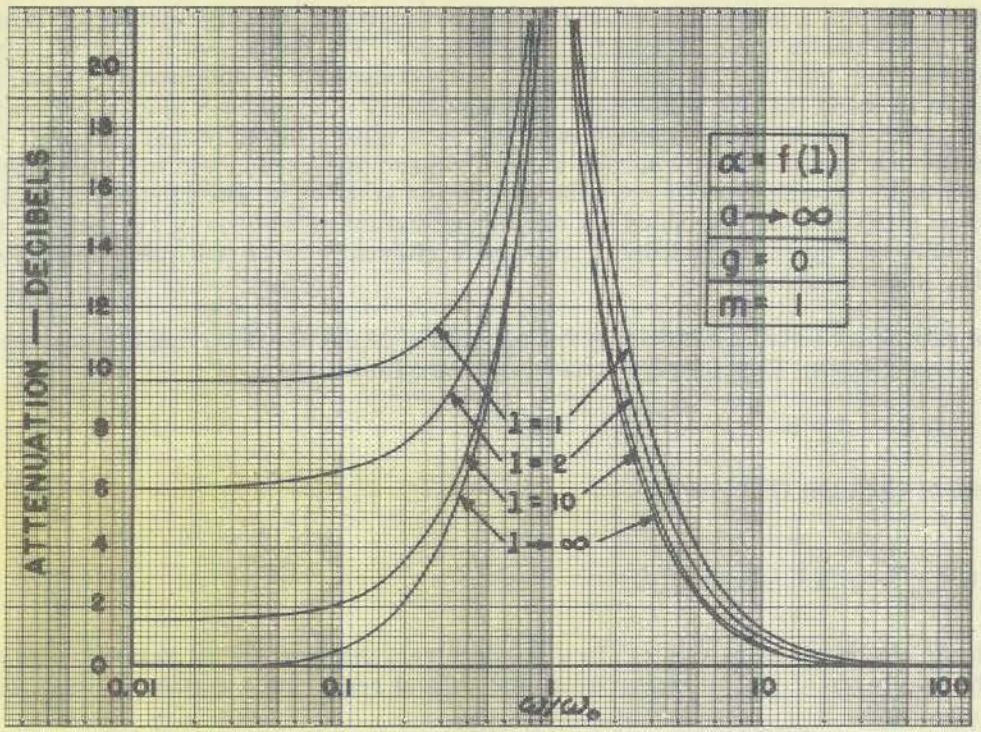

Fig. 19 - Load Resistance Effects

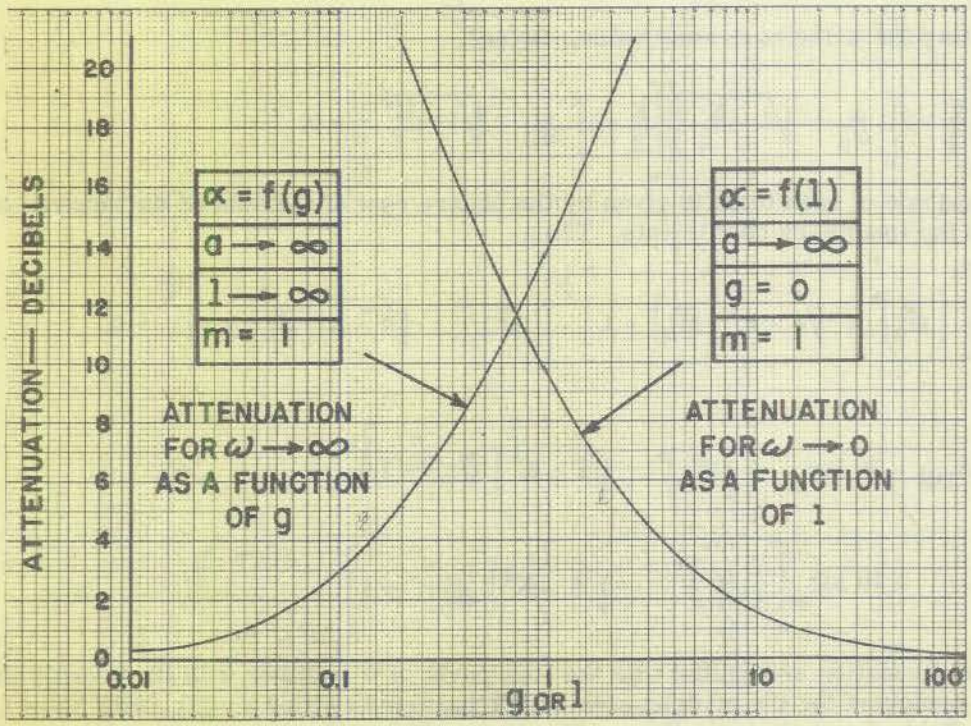

Fig. 20 - Generator and Load Resistance Parameter Selection - Design Data

Upon substitution of a particular value for the parameter a, the expression for α becomes the ratio of two quadratics with constant coefficients. The denominator has two negative real roots and the typical "low-pass filter" characteristics are obtained for these factors. However, it is found that the numerator is composed of a complex conjugate pair with negative real parts. One of the pair exhibits a characteristic similar to that shown in Figure 13 (asymptotic to a line of zero db/decade slope and zero attenuation and to a line of plus 20 db/decade slope passing through zero db attenuation at $\omega = \omega_0$). The other of the pair has the asymptotes just described but does not drop to minus infinity at $\omega = \omega_0$ as does the corresponding curve of Figure 13; instead, a maximum attenuation of finite value controlled by the value of a appears near $\omega = \omega_0$.

The procedure used in evaluating the magnitude of each of the complex conjugate factors is as follows: Consider an equation of the general form

$$u^2 + Ku + 1 = 0. \tag{17}$$

The roots of equation (17) are

$$u = -\frac{K}{2} \pm j \sqrt{1 - \frac{K^2}{4}} \tag{18}$$

in which the discriminant, $1 - (K^2/4)$, is a positive real number for all values of $|K| \leq 2$. Write the two parts of (18) in factor form and collect reals and imaginaries as follows:

$$\left[u + \frac{K}{2} - j \sqrt{1 - \frac{K^2}{4}}\right]\left[u + \frac{K}{2} + j \sqrt{1 - \frac{K^2}{4}}\right] = 0. \tag{19}$$

Substituting for u the equivalent value, $j(\omega/\omega_0)$,

$$\left[\frac{K}{2} + j\left[\frac{\omega}{\omega_0} + \sqrt{1 - \frac{K^2}{4}}\right]\right]\left[\frac{K}{2} + j\left[\frac{\omega}{\omega_0} - \sqrt{1 - \frac{K^2}{4}}\right]\right] = 0. \tag{20}$$

The magnitude of each term is given by the square root of the sum of the squares of the real and the imaginary coefficients. Thus,

$$\left[\left[\frac{\omega}{\omega_0}\right]^2 + \sqrt{4 - K^2}\left[\frac{\omega}{\omega_0}\right] + 1\right]^{\frac{1}{2}}\left[\left[\frac{\omega}{\omega_0}\right]^2 - \sqrt{4 - K^2}\left[\frac{\omega}{\omega_0}\right] + 1\right]^{\frac{1}{2}} = 0. \tag{21}$$

Finally,

$$A_{DB} = 10 \log_{10}\left[\left[\frac{\omega}{\omega_0}\right]^2 + \sqrt{4 - K^2}\left[\frac{\omega}{\omega_0}\right] + 1\right] + 10 \log_{10}\left[\left[\frac{\omega}{\omega_0}\right]^2 - \sqrt{4 - K^2}\left[\frac{\omega}{\omega_0}\right] + 1\right]. \tag{22}$$

The attenuation associated with the four parts of α together with the overall characteristic computed for the bridging-resistance parameter value a = 10, (with $l \to \infty$), are given in Table 5 and shown in Figure 21. Figure 22 is a family of curves showing the effect

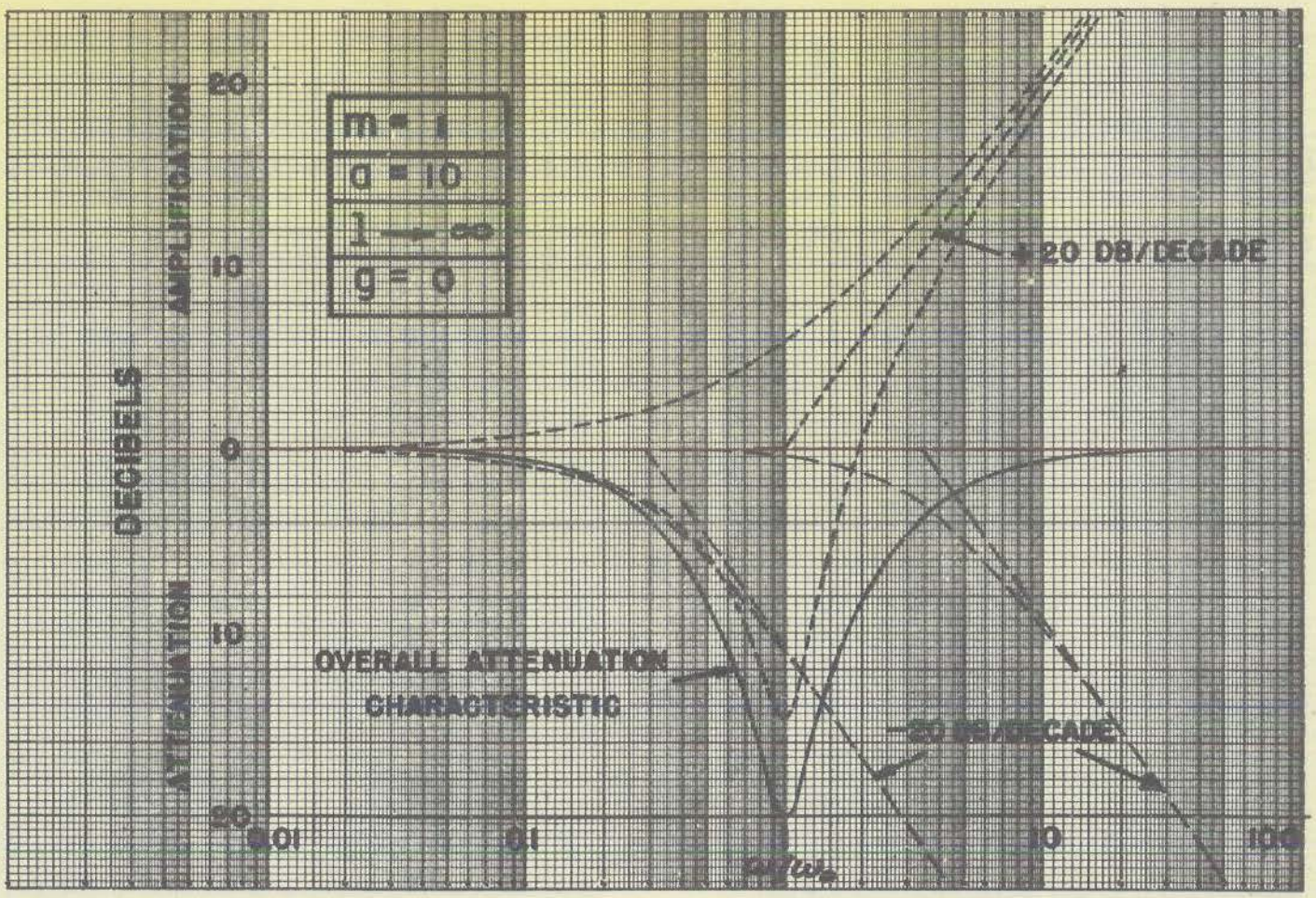

Fig. 21 - Bridged Network Attenuation Characteristics

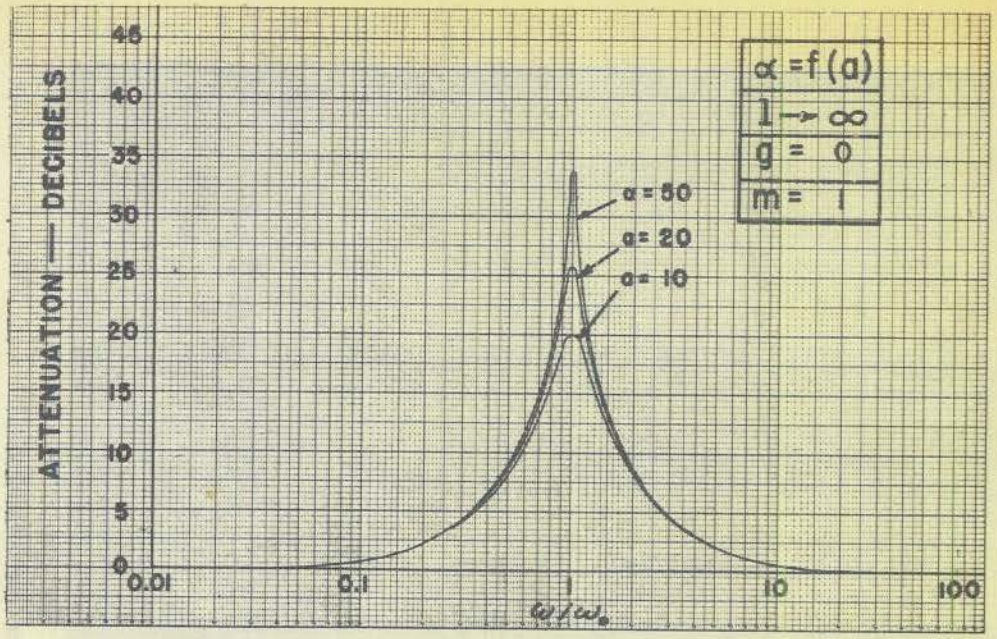

Fig. 22 - Bridging Resistance Effects for Infinite Load Resistance

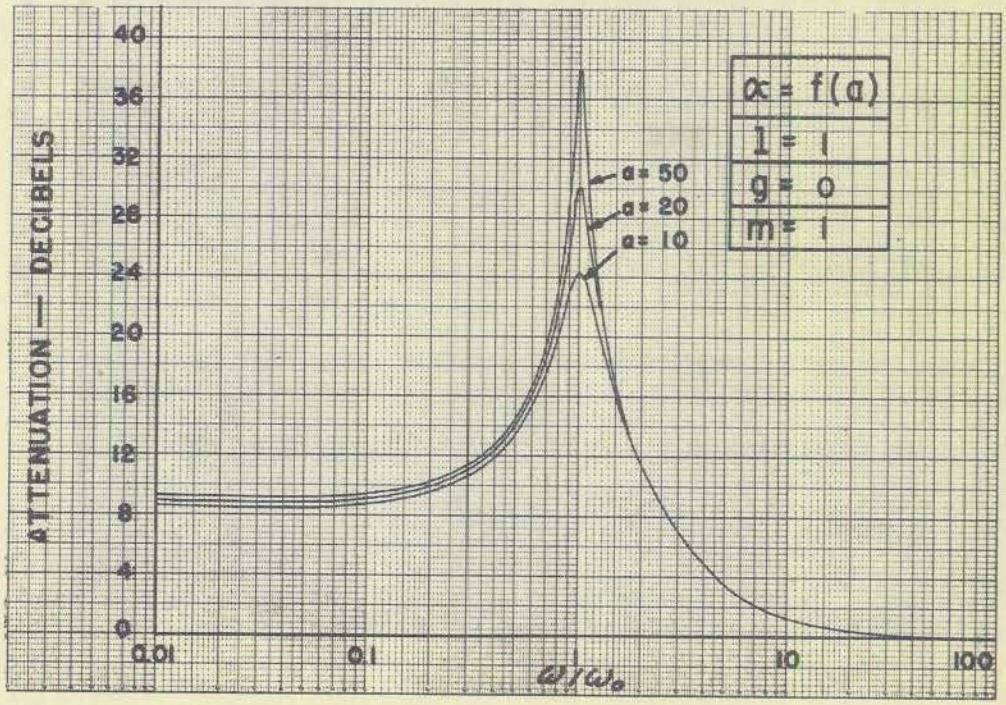

Fig. 23 - Bridging Resistance Effects for Finite Load Resistance

of varying the value of a (data in Table 6). Note that for reasonably large values of a, the effects due to bridging are essentially confined to the region of maximum attenuation.

Equation (15) reduces to the following for the finite load resistance specified by $l = 1$:

$$\alpha = \left[\frac{2+a}{2+3a}\right] \frac{\left[u^2 + u\left[\frac{4}{a}\cdot\frac{1+a}{2+a}\right] + 1\right]}{\left[u^2\left[\frac{2+a}{2+3a}\right] + u\left[\frac{6a^2+8a+4}{3a^2+2a}\right] + 1\right]} \cdot \qquad (23)$$

A family of curves for various values of a based on equation (23) is given in Figure 23 (data in Table 7). A comparison of the peak attenuations for the same value of a as shown in Figures 22 and 23 indicates that this important value is sensitive to the magnitude of both l and a. As a design aid, data for the curves of Figure 24 have been computed to aid in simultaneous selection of the maximum attenuation value and the values of the load resistance and the bridging resistance.

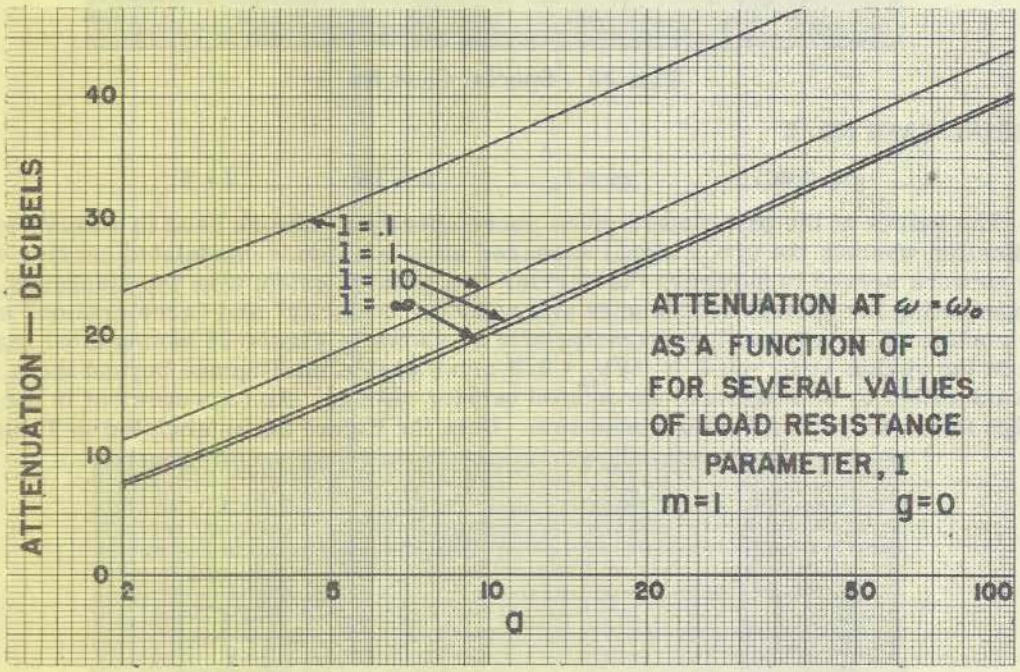

Fig. 24 - Peak Attenuation - Design Data

SPECIAL CASE NO. 1

$$g = 0.01, \qquad m = 10, \qquad a \to \infty, \qquad l = 100$$

Without unusual effort in a practical application of the network, it is possible to achieve the values of generator and load resistance specified by $g = 0.01$ and $l = 100$. It is also feasible to produce a network designed with $m = 10$. The application here involved no bridging resistance, and the transfer characteristic obtained shows nearly the upper limit of selectivity that may be expected experimentally. The attenuation characteristic is plotted in Figure 25 and data tabulated in Table 8.

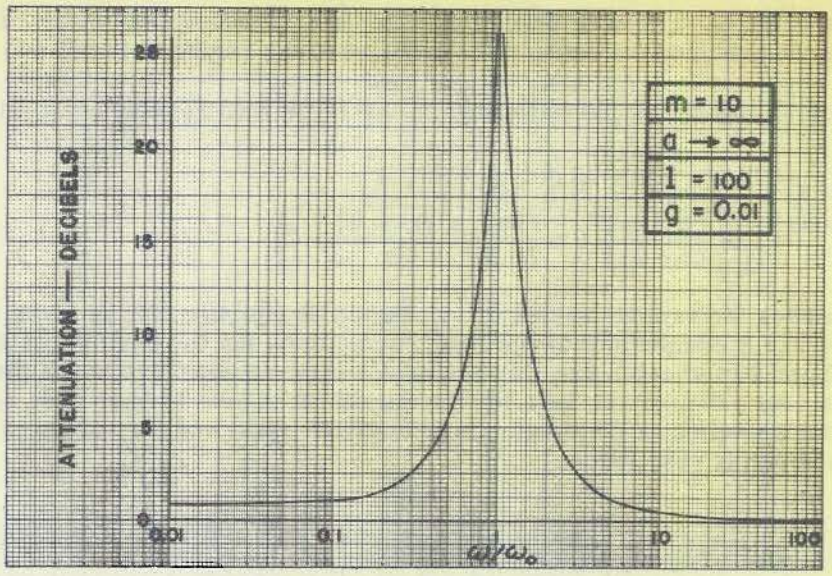

Fig. 25 - Special Case No. 1

SPECIAL CASE NO. 2

$g = 0.001, \qquad m = 1, \qquad a = 15 \qquad l = 2$

The values of the parameters given above specify a network used in a servo system application wherein the error signal appeared as an amplitude-modulated carrier voltage. The network served to suppress the carrier to a greater extent than the sidebands, thereby compensating for system deficiencies and reducing "velocity" and "acceleration" errors. The portion of the attenuation characteristic as shown in Figure 26 having most importance lies in the region $\omega/\omega_0 = 1/2$ to $\omega/\omega_0 = 3/2$ as no usable intelligence beyond these limits is transmitted by an amplitude-modulated carrier voltage. An improvement in the above design is the subject of a later discussion. Data for Figure 26 is tabulated in Table 8.

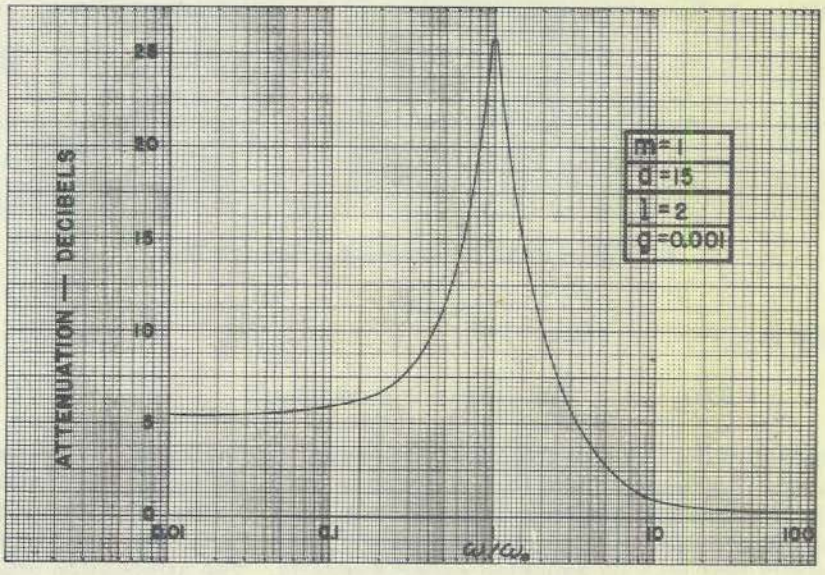

Fig. 26 - Special Case No. 2

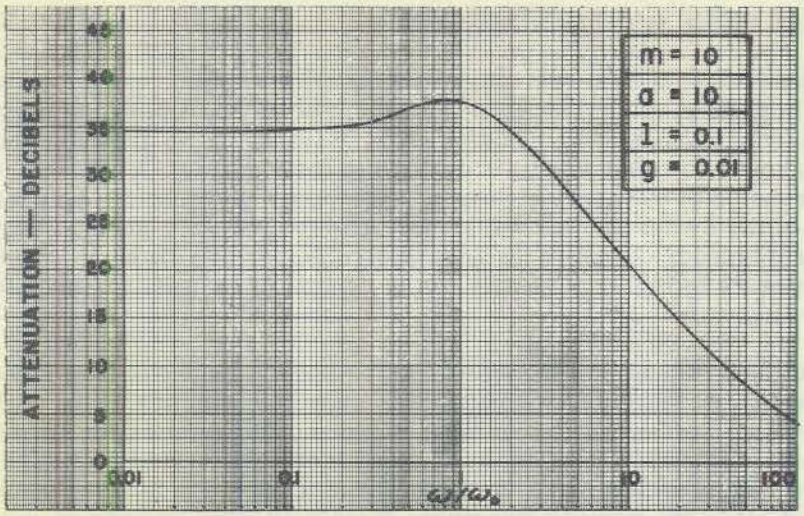

Fig. 27 - Special Case No. 3

SPECIAL CASE NO. 3

g = 0.01, m = 10, a = 10, l = 0.1

Extreme values of the parameters lead to wide variation from the null-type characteristic usually associated with a parallel-T network, and in special instances the added circuit complication may be justified. An illustration is that of Figure 27 plotted from data tabulated in Table 8. In this case, the shift in the frequency of maximum attenuation occurring for all cases where $g \neq 0$ and $l \not\to \infty$ is apparent.

SPECIAL CASE NO. 4

g = 0.001, m = 1, a = 40, l = 5

Network-response calculations for the above case were made in connection with a design for a selective amplifier wherein a bridged parallel-T was used to provide a narrow band pass rather than response to a single frequency. The attenuation characteristic is given by Figure 28 from data in Table 8.

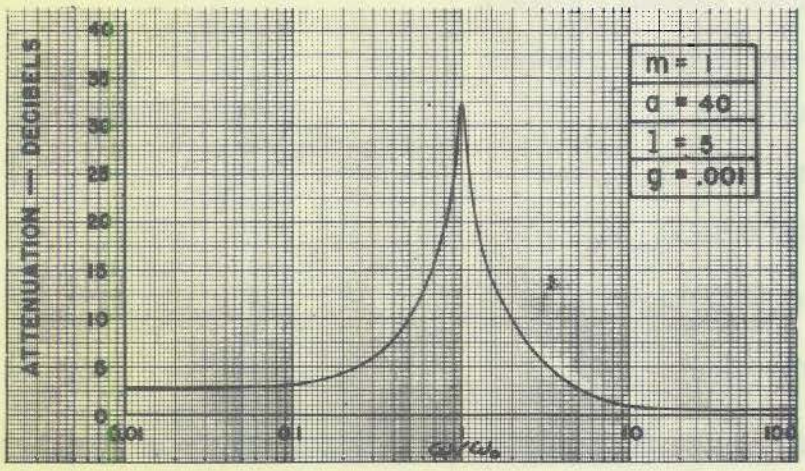

Fig. 28 - Special Case No. 4

SYMMETRICAL SIDEBAND TRANSMISSION

The bridged parallel-T network has been found to exhibit a transmission characteristic that is, in general, suited to servo system applications where the servo system employs a modulated carrier data-transmission system. If the frequency of maximum attenuation is made to coincide with the servo system carrier frequency, the resulting greater suppression at the carrier than at sideband frequencies can be used to equalize the response of the system to these sidebands and to produce a general improvement in servo system frequency response. A symmetrical upper and lower sideband transmission through the network is highly desirable, as is control of the relative magnitude of carrier and sideband attenuation.

A study of the attenuation characteristic for special case No. 2 as shown in Figure 26 reveals a greater attenuation for frequencies above ω_0 than for those a corresponding number of cycles below ω_0. A change in the values of the network parameters that results in an increased attenuation for $\omega < \omega_0$ and a decreased attenuation for $\omega > \omega_0$ is needed. From consideration of Figures 18 and 19, it is noted that a decrease in the value of either l or g produces an effect in the desired direction. Zero generator resistance can be approached experimentally and will be assumed. If m is set equal to unity, there remains the determination of suitable values for l for several values of a. Equation (15) applies for the stated conditions. Repeating,

$$\alpha = f(l,\ a), \qquad g = 0, \qquad m = 1$$

$$\alpha = \frac{u^2 + u\left[\frac{4}{a} \cdot \frac{a+1}{a+2}\right] + 1}{u^2 + u\left[\frac{4}{a} \cdot \frac{a+1}{a+2} + \frac{4a}{a+2} + \frac{2}{l}\right] + \left[1 + \frac{2}{l} \cdot \frac{a}{a+2}\right]} \tag{15}$$

To rearrange equation (15) to a suitable form, first let

ω_c = carrier frequency, radians/second,

ω_s = sideband frequency,

ω_{s1} = lower sideband frequency,

ω_{s2} = upper sideband frequency,

s = the ratio ω_s/ω_c,

s_1 = the ratio ω_{s1}/ω_c, and

s_2 = the ratio ω_{s2}/ω_c.

In equation (15), the variable

$$u = pCR = j\frac{\omega}{\omega_0} = j\frac{\omega_s}{\omega_c} = js \tag{24}$$

at any particular modulation frequency. If js is substituted for u in equation (15),

$$\alpha = \frac{\left[1 - s^2\right] + j\left[\frac{4}{a} \cdot \frac{1+a}{2+a}\right] s}{\left[1 + \frac{2a}{l(2+a)} - s^2\right] + j\left[\frac{4}{a} \cdot \frac{1+a}{2+a} + \frac{4a}{2+a} + \frac{2}{l}\right] s} \tag{25}$$

The attenuation implicit in equation (25) is given by

$$|\alpha| = \left[\frac{1 - 2s^2 + s^4 + \frac{16}{a^2}\left[\frac{1+a}{2+a}\right]^2 s^2}{\left[1 + \frac{2a}{l(2+a)}\right]^2 - 2\left[1 + \frac{2a}{l(2+a)}\right] s^2 + s^4 + \left[\frac{4}{a} \cdot \frac{1+a}{2+a} + \frac{4a}{2+a} + \frac{2}{l}\right]^2 s^2}\right]^{\frac{1}{2}} \tag{26}$$

Define

$$\delta = \frac{16}{a^2}\left[\frac{1+a}{2+a}\right]^2 - 2,$$

$$\zeta = \left[\frac{4}{a} \cdot \frac{1+a}{2+a} + \frac{4a}{2+a} + \frac{2}{l}\right]^2 - 2\left[1 + \frac{2a}{l(2+a)}\right],$$

$$\xi = \left[1 + \frac{2a}{l(2+a)}\right]^2,$$

and rewrite equation (26) to read

$$|\alpha| = \frac{\left[s^4 + \delta s^2 + 1\right]^{\frac{1}{2}}}{\left[s^4 + \zeta s^2 + \xi\right]^{\frac{1}{2}}}. \tag{27}$$

We desire equal attenuation at a given number of cycles below and the same number above the carrier frequency. Accordingly, for

$$|\alpha|_{s_1} = |\alpha|_{s_2},$$

$$\left[s_1^4 + \delta s_1^2 + 1\right] \cdot \left[s_2^4 + \zeta s_2^2 + \xi\right] = \left[s_2^4 + \delta s_2^2 + 1\right] \cdot \left[s_1^4 + \zeta s_1^2 + \xi\right]. \tag{28}$$

If the value of the parameter a is specified, the coefficients δ, ζ, and ξ become functions of l. Then, after specification of s_1 and s_2, equation (28) contains only constants and the parameter l. Pairs of values for a and l may be found in this manner.

On the presumption of a 60-cycle carrier, a suitable value of modulation frequency is 10 cycles per second. On this basis,

$$s_1 = \frac{50}{60}, \qquad s_2 = \frac{70}{60}. \tag{29}$$

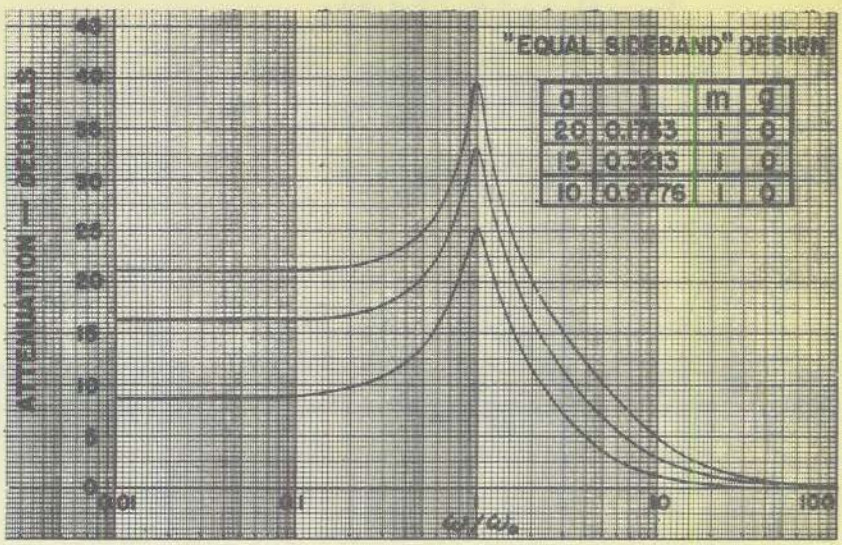

Fig. 29 - Equal Sideband Designs

Three pairs of values for a and l were computed and the corresponding attenuation data compiled (Table 9 and Figure 29). The special features of the network characteristics shown by the curves of Figure 29 are not well displayed by a logarithmic abscissa scale. When the curves are plotted with a linear scale for ω/ω_0 (Figure 30), the exact equivalence for the upper and lower sideband attenuation at 10 cycles per second is apparent as is the excellent agreement over the general range from zero to approximately 15 cycles per second. In practical servo system applications of the bridged parallel-T, the characteristic shown for the upper curve is more desirable than that corresponding to the others, although for the upper curve the attenuation is much greater at all frequencies. The greater attenuation at all frequencies does not make the design unusable since additional amplification at all frequencies is usually easily obtainable.

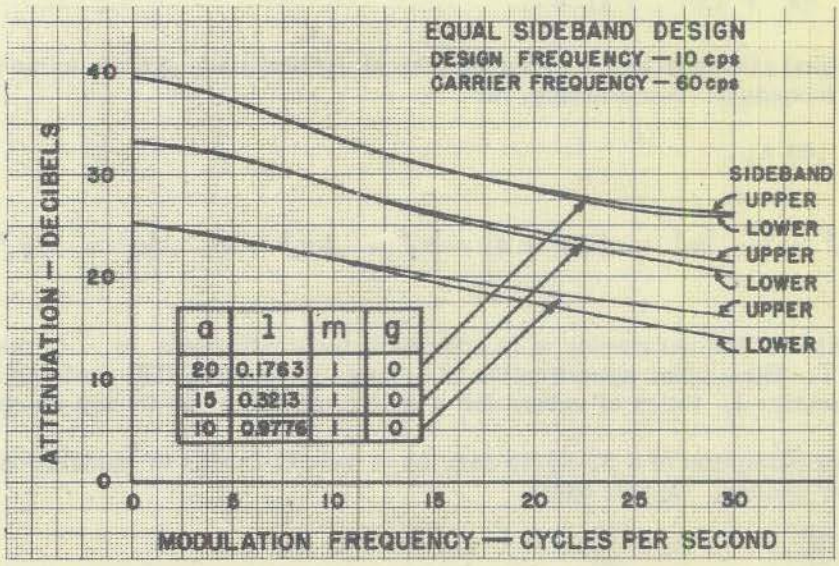

Fig. 30 - Symmetrical Sideband Designs Shown on Linear Modulation Frequency Scale

PRACTICAL DEVIATIONS FROM DESIGN VALUES

Successful practical realization of a selected transfer characteristic requires the procurement of a relatively large number of components, each within close tolerance of the calculated design value. The basic parallel-T network in its most general form is shown in Figure 31.

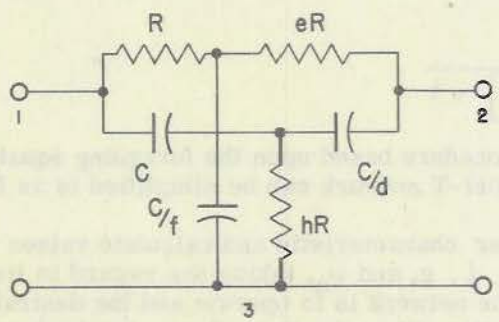

Fig. 31 - Generalized Parallel-T Network

In terms of the R and C at the input terminal, 1, and the parameters d, e, f, and h, the transfer characteristic is given by

$$\alpha = \frac{u^3 \frac{eh}{df} + u^2 \frac{h}{d}(e+1) + u \frac{h}{d}(d+1) + 1}{u^3 \frac{eh}{df} + u^2 \left[\frac{h}{d}(e+1) + \frac{h}{f}\left[\frac{d+1}{d}\right] + \frac{e}{df}\right] + u\left[\frac{1}{f} + h\left[\frac{d+1}{d}\right] + \frac{e+1}{d}\right] + 1} \tag{30}$$

where $u = pCR = j\omega CR$. The details of the derivation of equation (30) are given in Appendix IV. The conditions for a null are found by setting the real and the imaginary parts of the numerator of equation (30) each equal to zero. The resulting relations are

$$\omega_o = \frac{1}{CR}\sqrt{\frac{d}{h(e+1)}}, \tag{31}$$

and

$$\omega_o = \frac{1}{CR}\sqrt{\frac{f(d+1)}{e}}. \tag{32}$$

To obtain the desired specification of ω_o equal to 1/CR, it is necessary that

$$h = \frac{d}{e+1} \tag{33}$$

and

$$f = \frac{e}{d+1}. \tag{34}$$

For the values of h and f given in equations (33) and (34), the transfer characteristic given by equation (30) reduces to

$$\alpha = \frac{u^2 + 1}{u^2 + u\left[\frac{e+1}{d} + \frac{d+1}{e}\right] + 1}, \tag{35}$$

or

$$\alpha = \frac{u^2 + 1}{u^2 + u\left[\frac{f+h}{fh}\right] + 1}. \tag{36}$$

A straightforward procedure based upon the foregoing equations by which the construction of the null parallel-T network can be simplified is as follows:

Step 1. Select transfer characteristic and calculate values of R and C from the specified values of m, a, l, g, and ω_0, taking due regard to limitations imposed by the circuit within which the network is to operate and the desirability of small physical size of components. Usually, either the R or C may be obtained as a single unit and the other trimmed to meet the frequency requirement.

Step 2. Obtain components as conveniently near the calculated values of eR and C/d as possible and from measurements of the components, compute e and d.

Step 3. Use the formulas $h = \frac{d}{e+1}$ and $f = \frac{e}{d+1}$ to compute the values required for the components C/f and hR.

The above procedure reduces the number of components that must be made a specific value from six to three.

CONCLUSIONS

The bridged parallel-T network, a passive resistance-capacitance network operated between a generator having resistance and a resistance load, has been analyzed and the steady-state frequency-response characteristics have been shown by equations and families of curves. The effects of the four parameters consisting of network-symmetry parameter, bridging-resistance parameter, generator-resistance parameter, and load-resistance parameter have been explored and special cases studied in the presentation of the general theory of the network performance. A new design in which the upper and lower sideband transmission characteristics are matched has been developed for application in suppressed-carrier servo systems. A procedure for use in the practical construction of parallel-T networks has been given. From the study reported here it is concluded that by proper design the bridged parallel-T network may exhibit any of a wide range of desirable transfer characteristics.

ACKNOWLEDGEMENTS

The writer is pleased to acknowledge the interest and assistance of members of Radio Division III, Naval Research Laboratory. L. O. Brown, Jr., P. T. Stine, and M. S. McVay have kindly reviewed various portions of the work. The entire manuscript was read by Dr. D. C. Harkin and the group directed by D. O. Larson assisted with the computations.

REFERENCES

1. Herbert W. Augustadt, Electric Filter, U. S. Patent, No. 2,106,785, February 1, 1938. Application dated May 23, 1936.

2. H. H. Scott, "A New Type of Selective Circuit and Some Applications," Proc. I.R.E., Vol. 26, pp. 226-235, February 1938.

3. L. A. Meacham, "The Bridge-Stabilized Oscillator," Proc. I.R.E., Vol. 26, pp. 1278-1295, October 1938.

4. H. H. Scott, "An Analyzer for Noise Measurements," Gen. Rad. Exp., Vol. 13, pp. 6-11, February 1939.

5. W. N. Tuttle, "Bridged-T and Parallel-T Null Circuits for Measurements at Radio Frequencies," Proc. I.R.E., Vol. 28, p. 23, January 1940.

6. Mathematics Tables Project, Characteristics of Resistance Capacitance Electrical Networks, 50 Church St., New York, N. Y., March 25, 1942.

7. H. H. Scott, "An Analyzer for Sub-Audible Frequencies," Jour. Acoustical Soc. Amer., Vol. 13, pp. 360-362, April 1942.

8. W. G. Shepherd and R. O. Wise, "Variable-Frequency Bridge-Type Frequency-Stabilized Oscillator," Proc. I.R.E., Vol. 31, pp. 256-269, June 1943.

9. Ellison S. Purington, Universal Resistance Capacitance Filter, U. S. Patent, No. 2,354,141, July 18, 1944.

10. G. J. Thiessen, "R-C Filter Circuits," Jour. Acoustical Soc. Amer., Vol. 16, pp. 275-279, April 1945.

11. A. E. Hastings, "Analysis of a Resistance-Capacitance Parallel-T Network and Applications," Proc. I.R.E., Vol. 34, pp. 126P-129P, March 1946.

    R. M. Ashby, F. W. Martin, J. L. Lawson, "Modulation of Radar Signals from Airplanes," Radiation Laboratory Report No. 914 (Unpublished), March 28, 1946.

12. H. S. McGaughan, "A Variation of an R-C Parallel-T Network," Paper No. 42, Presented at URSI-IRE Joint Meeting, Wash., D. C., May 1946.

13. Leonard Stanton, "Theory and Application of Parallel-T Resistance-Capacitance Frequency-Selective Networks," Proc. I.R.E. Vol. 34, pp. 447-456, July 1946.

14. Alfred Wolf, "Note on a Parallel-T Resistance-Capacitance Network," Proc. I.R.E., Vol. 34, p. 659, September 1946.

15. J. R. Tillman, "Linear Frequency Discriminator," Wireless Engineer, Vol. 23, pp. 281-286, October 1946.

16. Jack L. Bowers, "R-C Bandpass Filter Design," Electronics, Vol. 20, pp. 131-133, April 1947.

APPENDIX I
ESTABLISHMENT OF NULL CRITERIA

From general network theory, the T-to-π conversion formulas by which Z_a, Z_b, and Z_c may be computed are

$$Z_a Z_2 = Z_b Z_3 = Z_c Z_1 = Z_1 Z_2 + Z_2 Z_3 + Z_1 Z_3. \tag{37}$$

From equation (4) it is seen that only the quantities entering into Z_β and Z_γ are needed. Proceeding,

$$Z_b = \frac{mR^2 + (m+1)\,R\,\frac{n}{pC}}{\frac{n}{pC}},$$

$$= (m+1)\left[1 + pCR\,\frac{m}{n(m+1)}\right]R. \tag{38}$$

$$Z_b' = \frac{\frac{m}{p^2C^2} + \frac{m+1}{pC}\cdot nR}{nR},$$

$$= \frac{m}{n}\left[\frac{1 + pCR\,\frac{n(m+1)}{m}}{p^2C^2R^2}\right]R. \tag{39}$$

The paralleled combination of Z_b and Z_b' is found as follows:

$$\frac{R}{Z_\beta} = \frac{1}{(m+1)\left[1 + pCR\,\frac{m}{n(m+1)}\right]} + \frac{\frac{n}{m}\,p^2C^2R^2}{1 + pCR\,\frac{n(m+1)}{m}},$$

$$Z_\beta = \frac{(m+1)\left[1 + pCR\,\frac{m}{n(m+1)}\right]\left[1 + pCR\,\frac{n(m+1)}{m}\right]R}{p^3C^3R^3 + p^2C^2R^2\,\frac{n(m+1)}{m} + pCR\,\frac{n(m+1)}{m} + 1}. \tag{40}$$

Again, using equations (37), we find

$$Z_c = \frac{m R^2 + (m+1) R \frac{n}{pC}}{R},$$

$$= n(m+1) \frac{\left[1 + pCR \frac{m}{n(m+1)}\right]}{pCR} R . \tag{41}$$

$$Z'_c = \frac{\frac{m}{p^2C^2} + \frac{m+1}{pC} \cdot nR}{\frac{1}{pC}},$$

$$= m \frac{1 + pCR \frac{n(m+1)}{m}}{pCR} R . \tag{42}$$

The paralleled combination of Z_c and Z'_c, which is Z_γ, is found as follows:

$$\frac{R}{Z_\gamma} = \frac{\frac{pCR}{n(m+1)}}{1 + pCR \frac{m}{n(m+1)}} + \frac{\frac{pCR}{m}}{1 + pCR \frac{n(m+1)}{m}},$$

$$Z_\gamma = \frac{\left[1 + pCR \cdot \frac{m}{n(m+1)}\right]\left[1 + pCR \cdot \frac{n(m+1)}{m}\right] \cdot R}{pCR\left[\frac{1}{m} + \frac{1}{n(m+1)}\right]\left[1 + pCR\right]} . \tag{43}$$

From equation (4), we see that the product of the numerator of equation (43) and the denominator of equation (40) is to be set equal to zero. Accordingly,

$$\left[1 + pCR \cdot \frac{m}{n(m+1)}\right] \cdot \left[1 + pCR \frac{n(m+1)}{m}\right] \cdot \left[p^3C^3R^3 + p^2C^2R^2 \frac{n(m+1)}{m} + pCR \frac{n(m+1)}{m} + 1\right] = 0 \tag{44}$$

Setting

$$pCR = j\left[\frac{\omega}{\omega_o}\right] = j, \tag{45}$$

equation (44) reduces to

$$\left[1 + j\frac{m}{n(m+1)}\right]\left[1 + j\frac{n(m+1)}{m}\right]\left[1 - \frac{n(m+1)}{m} + j\frac{n(m+1) - m}{m}\right] = 0. \tag{46}$$

Both the real and the imaginary components reduce to

$$\frac{n^2(m+1)^2}{m^2} - \frac{n(m+1)}{m} + 1 - \frac{m}{n(m+1)} \tag{47}$$

which is equal to zero for

$$n = \frac{m}{m+1} .$$

APPENDIX II
DETERMINATION OF RETUNING-RESISTANCE PARAMETER

The two T configurations of Figure 11 may be separately converted to equivalent-π sections using the formulas of (37) and Figures 32 and 33.

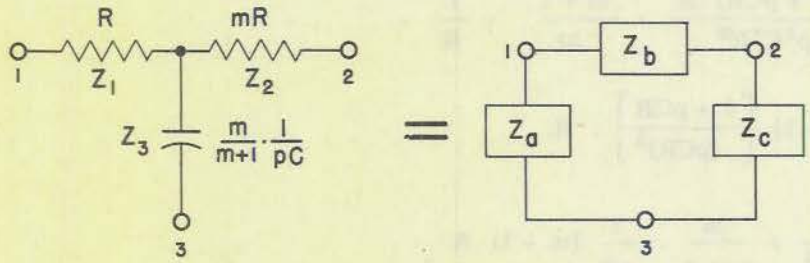

Fig. 32 - Two-Resistor T-to-π Transformation

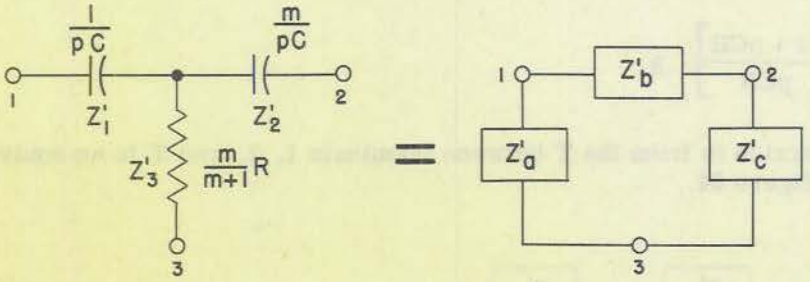

Fig. 33 - Two-Condenser T-to-π Transformation

For the T of Figure 32:

$$Z_a = \left[m R^2 + \frac{m}{m+1} \cdot \frac{1}{pC} \quad (m+1)\ R \right] \frac{1}{mR} ,$$

$$= \frac{1 + pCR}{pCR} . R . \tag{48}$$

$$Z_b = \frac{m \left[\frac{1 + pCR}{pCR} \right] R^2}{\frac{m}{m+1} \cdot \frac{1}{pC}} , \quad = (m+1)(1 + pCR)\ R. \tag{49}$$

$$Z_c = m\left[\frac{1 + pCR}{pCR}\right] \cdot R. \tag{50}$$

For the T of Figure 33:

$$Z'_a = \frac{\frac{m}{p^2C^2} + \frac{m}{m+1} \cdot \frac{1}{pC}(m+1)R}{\frac{m}{pC}},$$

$$= \left[\frac{1 + pCR}{pCR}\right] \cdot R. \tag{51}$$

$$Z'_b = \frac{m(1 + pCR)\ R^2}{p^2C^2R^2} \cdot \frac{m+1}{m} \cdot \frac{1}{R},$$

$$= (m+1) \cdot \left[\frac{1 + pCR}{(pCR)^2}\right] \cdot R. \tag{52}$$

$$Z'_c = \frac{\frac{m}{p^2C^2} + \frac{m}{m+1} \cdot \frac{1}{pC}(m+1)\ R}{\frac{1}{pC}},$$

$$= m\left[\frac{1 + pCR}{pCR}\right] \cdot R. \tag{53}$$

The next conversion is from the T between terminals 1, 2, and 3' to an equivalent -π section. See Figure 34.

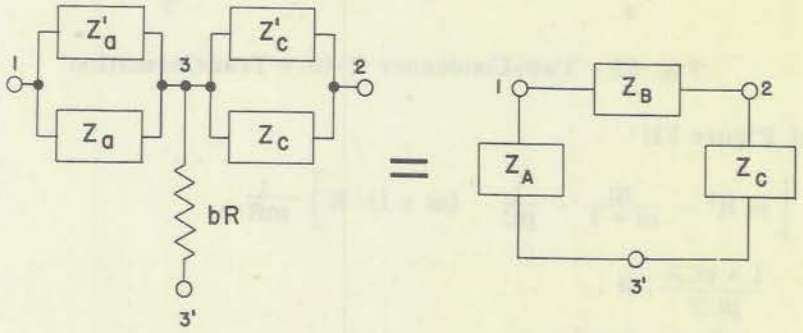

Fig. 34 - T-to-π Transformation Including b R

Thus,

$$Z_{13} = \frac{Z_a Z'_a}{Z_a + Z'_a} = \frac{1}{2}\left[\frac{1 + pCR}{pCR}\right] . R. \tag{54}$$

$$Z_{23} = \frac{Z_c Z'_c}{Z_c + Z'_c} = \frac{m}{2}\left[\frac{1 + pCR}{pCR}\right] . R. \tag{55}$$

$$Z_{33'} = bR. \tag{56}$$

The T-to-π conversion formulas are similar to equations (37) as follows:

$$Z_A Z_{23} = Z_B Z_{33'} = Z_C Z_{13} = Z_{13} Z_{23} + Z_{23} Z_{3'3} + Z_{13} Z_{3'3} . \tag{57}$$

Solving for Z_A, Z_B, and Z_C we have

$$Z_A = \left[\frac{1}{2}\left[\frac{1 + pCR}{pCR}\right] + b\,\frac{m + 1}{m}\right] R \tag{58}$$

$$Z_B = \left[\frac{m}{4b}\left[\frac{1 + pCR}{pCR}\right]^2 + \frac{m + 1}{2}\left[\frac{1 + pCR}{pCR}\right]\right] R ,$$

$$= \frac{m}{4b}\left\{\frac{(1 + pCR)\left[1 + pCR\left[1 + 2b\,\frac{m + 1}{m}\right]\right]}{(pCR)^2}\right\} R. \tag{59}$$

$$Z_C = \left\{\frac{m}{2}\left[\frac{1 + pCR}{pCR}\right] + b\,(m + 1)\right\} R . \tag{60}$$

The circuit of Figure 11 has been converted to that shown at the left in Figure 35. The final conversion is to that shown at the right in this figure.

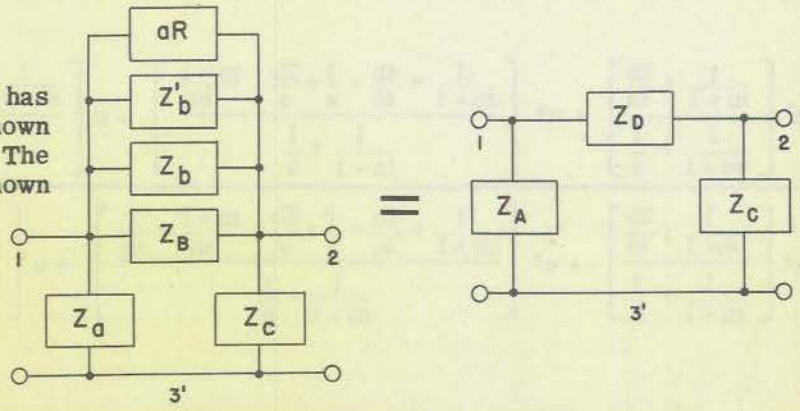

Fig. 35
Final Transformation

$$\frac{1}{Z_D} = \frac{1}{Z_B} + \frac{1}{Z_b} + \frac{1}{Z_b'} + \frac{1}{aR} \quad . \tag{61}$$

Substitution in equation (61) of the indicated quantities from equations (59), (49), and (52) gives

$$Z_D = (1 + pCR)\left[1 + pCR\left[1 + 2b\ \frac{m+1}{m}\right]\right] \Big/ \Delta \tag{62}$$

where

$$\Delta = p^3C^3R^3\left[\frac{1}{m+1} + \frac{2b}{m}\right] + p^2C^2R^2\left[\frac{4b}{m} + \frac{1}{m+1} + \frac{1}{a} + \frac{2b}{a}\cdot\frac{m+1}{m}\right]$$

$$+ pCR\left[\frac{1}{m+1} + \frac{2b}{m} + \frac{2}{a} + \frac{2b}{a}\cdot\frac{m+1}{m}\right] + \left[\frac{1}{m+1} + \frac{1}{a}\right] .$$

The transfer characteristic may be found from the expressions for Z_C and Z_D for

$$\alpha = \frac{E_{out}}{Ein} = \frac{Z_C}{Z_C + Z_D} = \frac{1}{1 + \frac{Z_D}{Z_C}} \tag{63}$$

Let $u = pCR$ and write

$$\alpha = \left\{1 + \left[(1+u)\left[1 + u\left[1 + 2b\ \frac{m+1}{m}\right]\right] \Big/ \Delta\right]\right\}^{-1} \tag{64}$$

where

$$\Delta = \left[b(m+1) + \frac{m}{2}\cdot\frac{1+u}{u}\right]\left[u^3\left[\frac{1}{m+1} + \frac{2b}{m}\right] + u^2\left[\frac{4b}{m} + \frac{1}{m+1} + \frac{1}{a} + \frac{2b}{a}\cdot\frac{m+1}{m}\right]\right.$$

$$\left. + u\left[\frac{1}{m+1} + \frac{2b}{m} + \frac{2}{a} + \frac{2b}{a}\cdot\frac{m+1}{m}\right] + \left[\frac{1}{m+1} + \frac{1}{a}\right]\right]$$

$$\alpha = \frac{u^3\left[\dfrac{\frac{1}{m+1} + \frac{2b}{m}}{\frac{1}{m+1} + \frac{1}{a}}\right] + u^2\left[\dfrac{\frac{1}{m+1} + \frac{4b}{m} + \frac{1}{a} + \frac{2b}{a}\cdot\frac{m+1}{m}}{\frac{1}{m+1} + \frac{1}{a}}\right] + u\left[\dfrac{\frac{1}{m+1} + \frac{2b}{m} + \frac{2}{a} + \frac{2b}{a}\cdot\frac{m+1}{m}}{\frac{1}{m+1} + \frac{1}{a}}\right] + 1}{u^3\left[\dfrac{\frac{1}{m+1} + \frac{2b}{m}}{\frac{1}{m+1} + \frac{1}{a}}\right] + u^2\left[\dfrac{\frac{1}{m+1} + \frac{4b}{m} + \frac{1}{a} + \frac{2b}{a}\cdot\frac{m+1}{m} + \frac{2}{m}}{\frac{1}{m+1} + \frac{1}{a}}\right] + u\left[\dfrac{\frac{1}{m+1} + \frac{2b}{m} + \frac{2}{a} + \frac{2b}{a}\cdot\frac{m+1}{m} + \frac{2}{m}}{\frac{1}{m+1} + \frac{1}{a}}\right] + 1} \tag{65}$$

As defined by equation (65), α is of the form

$$\alpha = \frac{A + jB}{C + jD} = \sqrt{\frac{A^2 + B^2}{C^2 + D^2}} \quad \angle \tan^{-1}\frac{B}{A} - \tan^{-1}\frac{D}{C} . \tag{66}$$

For $u = pCR = j\frac{\omega}{\omega_0} = j$ and zero phase shift,

$$\frac{B}{A} = \frac{D}{C} \quad \text{or} \quad CB = AD . \tag{67}$$

The equality indicated by equation (67), upon substitution of the corresponding terms from equation (65), becomes

$$\left[\frac{1}{m+1} + \frac{1}{a} - \frac{1}{m+1} - \frac{4b}{m} - \frac{1}{a} - \frac{2b}{a}\cdot\frac{m+1}{m} - \frac{2}{m}\right]\cdot\left[\frac{1}{m+1} + \frac{2b}{m} + \frac{2}{a} + \frac{2b}{a}\cdot\frac{m+1}{m} - \frac{1}{m+1} - \frac{2b}{m}\right]$$

$$= \left[\frac{1}{m+1} + \frac{1}{a} - \frac{1}{m+1} - \frac{4b}{m} - \frac{1}{a} - \frac{2b}{a}\cdot\frac{m+1}{m}\right]\cdot\left[\frac{1}{m+1} + \frac{2b}{m} + \frac{2}{a} + \frac{2b}{a}\cdot\frac{m+1}{m} + \frac{2}{m} - \frac{1}{m+1} - \frac{2b}{m}\right]. \tag{68}$$

From equation (68), the desired relationship is found to be

$$b = \frac{m}{2a} . \tag{6}$$

APPENDIX III

GENERAL EQUATION FOR TRANSFER CHARACTERISTIC

In Appendix II, an equivalent-π was derived that simplifies the determination of the transfer characteristic for the circuit of Figure 12. Based on Figure 36, the principle of successive voltage divider action is used to determine the ratio of the output voltage to the input voltage.

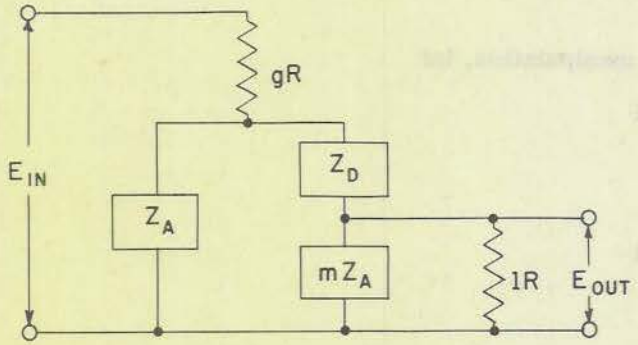

Fig. 36 - Circuit for Transfer-Equation Determination

Thus,

$$\alpha = \frac{E_{out}}{E_{in}} = \left\{ \frac{\frac{l Z_c}{l + Z_c}}{Z_D + \frac{l Z_c}{l + Z_c}} \right\} \left\{ \frac{\frac{Z_A \left[Z_D + \frac{l Z_c}{l + Z_c} \right]}{Z_A + Z_D + \frac{l Z_c}{l + Z_c}}}{g + \frac{Z_A \left[Z_D + \frac{l Z_c}{l + Z_c} \right]}{Z_A + Z_D + \frac{l Z_c}{l + Z_c}}} \right\} . \tag{69}$$

From equations (58) and (60) it is seen that

$$Z_C = m \cdot Z_A . \tag{70}$$

Equation (69) reduces to the form

$$\alpha = \frac{l\, m\, Z_A^2}{Z_A^2 \left[m(g + l + Z_D) \right] + Z_A \left[gl\,(m+1) + Z_D(gm + l) \right] + Z_D g\, l}, \tag{71}$$

into which the quantities Z_A and Z_D must be substituted. Replacing b by $\frac{m}{2a}$ in equations (58) and (62), we have

$$Z_A = \frac{1}{2} \left[\frac{1 + u \left[\frac{m+1+a}{a} \right]}{u} \right] \cdot R, \tag{72}$$

and

$$Z_D = \frac{1 + u \left[\frac{m+1+a}{a} \right]}{u^2 \left[\frac{m+1+a}{(m+1)a} \right] + u \left[\frac{m+1+2a}{a^2} \right] + \left[\frac{m+1+a}{(m+1)\,a} \right]} \; R. \tag{73}$$

For greater ease in manipulation, let

$$q = \frac{m+1+a}{a} \tag{74}$$

and write

$$Z_A = \frac{1 + uq}{2u} \cdot R \tag{75}$$

and

$$Z_D = \frac{m+1}{q} \cdot \frac{1 + uq}{u^2 + u \left[\frac{q+1}{q} \cdot \frac{m+1}{a} \right] + 1} \; R. \tag{76}$$

Straightforward substitution into equation (71), collection of terms, and replacement of substituted quantities with the equivalent forms in terms of the basic parameters of the circuit result in the transfer characteristic specified by equation (8).

APPENDIX IV

DERIVATION OF PRACTICAL DESIGN EQUATIONS

The transfer characteristic for the network of Figure 31 is obtained in a manner identical to that shown by Figures 8, 9, and 10 and by equation (1). See Appendix I for detailed procedure. For the network of Figure 31 the equivalent quantities are

$$Z_a = \left[\frac{1 + u \dfrac{e}{f(e+1)}}{u \dfrac{e}{f(e+1)}} \right] R \tag{77}$$

$$Z_b = (e+1) \left[1 + u \frac{e}{f(e+1)} \right] R \tag{78}$$

$$Z_c = e\, Z_a \tag{79}$$

$$Z'_a = \left[\frac{1 + u\, h \dfrac{d+1}{d}}{u} \right] R \tag{80}$$

$$Z'_b = \frac{d}{h} \left[\frac{1 + u\, h \left[\dfrac{d+1}{d} \right]}{u^2} \right] R \tag{81}$$

$$Z'_c = d\, Z'_a \tag{82}$$

Only the paralleled combinations of Z_β and Z_γ are needed. Thus:

$$Z_\beta = \frac{Z_b\, Z'_b}{Z_b + Z'_b}$$

$$Z_\beta = \frac{\left[1 + u \dfrac{e}{f(e+1)} \right] \left[1 + u\, h \dfrac{d+1}{d} \right]}{u^3 \dfrac{eh}{fd(e+1)} + u^2 \dfrac{h}{d} + u \dfrac{h(d+1)}{d(e+1)} + \dfrac{1}{e+1}} R \tag{83}$$

$$Z_\gamma = \frac{Z_C Z'_C}{Z_C + Z'_C}$$

$$Z_\gamma = \frac{\left[1 + u\frac{e}{f(e+1)}\right]\left[1 + u\,h\frac{d+1}{d}\right]}{u\left[\frac{1}{d} + \frac{1}{f(e+1)} + u\left[\frac{h(d+1)}{fd(e+1)} + \frac{e}{df(e+1)}\right]\right]} R. \tag{84}$$

The transfer characteristic is given by the following in which the N stands for numerator and the D stands for denominator:

$$\alpha = \frac{Z_\gamma}{Z_\gamma + Z_\beta} = \frac{\frac{Z_{\gamma N}}{Z_{\gamma D}}}{\frac{Z_{\gamma N}}{Z_{\gamma D}} + \frac{Z_{\beta N}}{Z_{\beta D}}} \tag{85}$$

Since the numerators of equations (83) and (84) are identical, we have

$$\alpha = \frac{Z_{\beta D}}{Z_{\beta D} + Z_{\gamma D}\left[\frac{Z_{\beta N}}{Z_{\gamma N}}\right]} = \frac{Z_{\beta D}}{Z_{\beta D} + Z_{\gamma D}} \tag{86}$$

and upon substitution,

$$\alpha = \frac{u^3\,\frac{eh}{fd} + u^2\,\frac{h}{d}(e+1) + u\,\frac{h}{d}(d+1) + 1}{u^3\,\frac{eh}{fd} + u^2\left[\frac{h}{d}(e+1) + \frac{h}{f}\left[\frac{d+1}{d}\right] + \frac{e}{df}\right] + u\left[\frac{h}{d}(d+1) + \frac{1}{f} + \frac{e+1}{d}\right] + 1} \tag{87}$$

Equation (87) is equation (30) of the text.

APPENDIX V
TABLES OF DATA

TABLE 1

Basic Terms for Un-Bridged Network

$1 + \omega/\omega_0$; $A_{DB} = 20 \log_{10} |1 + \omega/\omega_0|$, $B = 0$

$1 - \omega/\omega_0$; $A_{DB} = 20 \log_{10} |1 - \omega/\omega_0|$

$A_{DB} < 0$ for $\omega/\omega_0 < 2$ $\quad B = 0$ for $\omega/\omega_0 < 1$

$A_{DB} > 0$ for $\omega/\omega_0 > 2$ $\quad B = 180$ for $\omega/\omega_0 > 1$

$\frac{1}{1 + p/\omega_0}$; $A_{DB} = -10 \log_{10} |1 + (\omega/\omega_0)^2|$, $B = -\tan^{-1} (\omega/\omega_0)$

ω/ω_0	$(1 + \omega/\omega_0)$		$(1 - \omega/\omega_0)$		$(1 + p/\omega_0)^{-1}$	
	A_{DB}	B	A_{DB}	B	A_{DB}	B
.01	.086	0	- .087	0	- .0004	- 0.6
.05	.423		- .446		- .0026	- 2.8
.1	.828		- .915		- .0432	- 5.7
.2	1.584		- 1.619		- .1703	-11.3
.4	2.922		- 4.436		- .6445	-21.8
.5	3.522		- 6.021		- .9691	-26.5
.6	4.082		- 7.959		- 1.3353	-31.0
.7	4.616		-10.457		- 1.73186	-35.0
.8	5.105		-13.979		- 2.148	-38.7
.9	5.575		-20.000		- 2.577	-42.0
1	6.021		- ∞	0,180	- 3.0103	-45.0
1.2	6.848		-13.979		- 3.8739	-50.2
1.4	7.604		- 7.959		- 4.7129	-54.5
1.7	8.627		- 3.098		- 5.8995	-59.5
2	9.542		0		- 6.9897	-63.4
3	12.041		+ 6.021		-10.0000	-71.6
4	13.981		+ 9.542		-12.3045	-76.0
6	16.902		+13.979		-15.6820	-80.5
8	19.085		+16.902		-18.1291	-82.9
10	20.828		+19.085		-20.0432	-84.3
50	34.151		+33.804		-33.9794	-88.9
100	40.086	0	+39.000	180	-40.0004	-89.4

TABLE 2

Data for Figure 15, Based on Equation (10)

$\alpha = f(m)$, $\quad a \to \infty$, $\quad l \to \infty$, $\quad g = 0$

ω/ω_0	$m \to \infty$	m = 10	m = 1	m = .1
.01	.00	.00	.01	.20
.05	.04	.05	.04	3.46
.1	.17	.21	.65	7.75
.2	.69	.82	2.29	13.43
.4	2.71	3.02	6.55	20.36
.5	4.44	4.98	9.09	23.35
.6	6.58	7.20	11.78	26.31
.7	9.32	10.05	14.94	29.61
.8	13.17	13.96	19.03	33.79
.9	19.58	20.39	25.56	40.37
1	∞	∞	∞	∞
1.2	14.88	15.68	20.79	35.57
1.4	9.78	10.53	15.44	30.14
1.7	6.27	6.99	11.44	25.95
2	4.44	4.98	9.09	23.35
3	1.94	2.26	5.12	18.40
4	1.08	1.32	3.30	15.51
6	.48	.67	1.67	11.83
8	.27	.32	1.00	9.45
10	.17	.21	.65	7.75
50	.00	.01	.03	.78
100	.00	.00	.01	.20

TABLE 3

Data for Figure 18, Based on Equation (12)

$\alpha = f(g)$,	$a \to \infty$,	$l \to \infty$,	m = 1
ω/ω_0	g = .001	g = .1	g = .5
.01	.01	.01	.01
.05	.17	.20	.33
.1	.66	.75	1.23
.2	2.29	2.57	3.80
.4	6.56	7.10	9.22
.5	9.10	9.71	12.07
.6	11.79	12.46	15.01
.7	14.94	15.67	18.37
.8	19.03	19.81	22.65
.9	24.76	26.39	29.36
1	∞	∞	∞
1.2	20.80	21.64	25.11
1.4	15.45	16.48	20.10
1.7	11.45	12.62	16.59
2	9.10	10.40	14.67
3	5.13	6.83	11.95
4	3.32	5.33	10.92
6	1.70	4.08	10.17
8	1.03	3.59	9.90
10	.69	3.36	9.78
50	.06	2.93	9.55
100	.04	2.93	9.54

TABLE 4

Data for Figure 19, Based on Equation (14)

$\alpha = f(l)$,	$a \to \infty$,	g = 0,		m = 1
ω/ω_0	$l \to \infty$	l = 10	l = 2	l = 1
.01	.01	1.59	6.03	9.54
.05	.04	1.72	6.10	9.60
.1	.65	2.11	6.51	9.77
.2	2.29	3.47	7.46	10.44
.4	6.55	7.33	10.28	12.82
.5	9.09	9.75	12.37	14.69
.6	11.78	12.38	14.55	16.87
.7	14.94	15.47	17.49	19.64
.8	19.03	19.52	21.40	23.44
.9	25.56	26.02	27.78	29.73
1	∞	∞	∞	∞
1.2	20.79	21.19	22.73	24.48
1.4	15.44	15.82	17.26	18.89
1.7	11.44	12.89	13.11	14.64
2	9.09	9.40	10.63	12.07
3	5.12	5.35	6.32	7.50
4	3.30	3.48	4.23	5.20
6	1.67	1.78	2.25	2.89
8	1.00	1.07	1.37	1.81
10	.65	.70	.92	1.23
50	.03	.03	.04	.06
100	.01	.01	.01	.01

TABLE 5

Data for Figure 21, Based on Equation (16) with a = 10

$$\alpha = \frac{u^2 + u\ .190909 + 1}{u^2 + u\ 3.82727 + 1}$$

Numerator: K = .190909 (See Equation 22)
Denominator: (1 + p/.282)(1 + p/3.545)

a = 10, $l \to \infty$, g = 0, m = 1

ω/ω_0	Numerator DB 1st Term	Numerator DB 2nd Term	Denominator DB 1st Term	Denominator DB 2nd Term	α_{DB} (Minus)
.01	.08	- .09	- .00	- .05	.05
.05	.42	- .44	- .00	- .12	.15
.1	.82	- .90	- .00	- .48	.60
.2	1.56	- 1.89	- .02	- 1.66	2.00
.4	2.90	- 4.28	- .06	- 4.56	6.00
.5	3.49	- 5.74	- .09	- 5.91	8.25
.6	4.05	- 7.44	- .13	- 7.14	10.67
.7	4.57	- 9.44	- .18	- 8.25	13.30
.8	5.07	-11.73	- .24	- 9.26	16.15
.9	5.54	-13.92	- .33	-10.17	18.89
1	5.98	-14.69	- .36	-11.00	20.08
1.2	6.81	-10.93	- .51	-12.48	17.11
1.4	7.57	- 6.83	- .68	-13.76	13.70
1.7	8.59	- 2.62	- .97	-15.38	10.38
2.0	9.51	+ .28	- 1.29	-16.76	8.25
3.0	12.01	+ 6.13	- 2.49	-20.23	4.58
4.0	13.96	+ 9.61	- 3.76	-22.71	2.91
6.0	16.88	+14.01	- 6.13	-26.22	1.46
8.0	19.07	+15.93	- 8.14	-28.71	.86
10	20.82	+19.10	- 9.83	-30.65	.56
50	34.15	+33.81	-23.35	-44.63	.02
100	40.09	+39.91	-29.36	-50.65	.01

TABLE 6

Data for Figure 22, Based on Equation (16)

$\alpha = f(a)$,	$l \to \infty$,	g = 0,	m = 1
ω/ω_0	a = 50	a = 20	a = 10
.01	.01	.01	.05
.05	.17	.15	.15
.1	.62	.60	.60
.2	2.22	2.13	2.00
.4	6.52	6.32	6.00
.5	8.94	8.69	8.25
.6	11.60	11.29	10.67
.7	14.73	14.27	13.30
.8	18.74	17.94	16.15
.9	24.77	22.59	18.89
1	33.78	25.76	20.08
1.2	20.44	19.14	17.11
1.4	15.23	14.74	13.70
1.7	11.27	10.85	10.38
2	8.93	8.69	8.25
3	4.90	4.86	4.58
4	3.21	3.09	2.91
6	1.61	1.55	1.46
8	.96	.92	.86
10	.63	.60	.56
50	.02	.03	.02
100	.01	.01	.01

TABLE 7

Data for Figure 23, Based on Equation (23)

$\alpha = f(a)$,	$l = 1$,	g = 0,	m = 1
ω/ω_o	a = 10	a = 20	a = 50
.01	8.52	9.00	9.32
.05	8.58	9.06	9.37
.1	8.76	9.24	9.54
.2	9.47	9.93	10.23
.4	11.99	12.45	12.73
.5	13.70	14.22	14.51
.6	15.70	16.36	16.69
.7	18.02	18.99	19.82
.8	20.63	22.38	23.17
.9	23.13	26.82	29.03
1	24.19	30.10	37.99
1.2	20.96	23.15	24.16
1.4	17.34	18.31	18.73
1.7	13.75	14.26	14.51
2	11.41	11.76	11.96
3	7.08	7.28	7.40
4	4.87	5.02	5.13
6	2.68	2.78	2.84
8	1.69	1.73	1.78
10	1.13	1.17	1.20
50	.05	.05	.05
100	.01	.01	.00

TABLE 8

Special Cases No. 1, No. 2, No. 3, and No. 4

Fig.	25	26	27	28
m	10	1	10	1
a	∞	15	10	40
l	100	2	0.1	5
g	0.01	0.001	0.01	0.001
ω/ω_o	Attenuation in Decibels			
.01	0.91	5.50	34.52	2.81
.05	0.96	5.57	34.61	2.92
.1	1.10	5.81	34.73	3.24
.2	1.69	6.69	35.17	4.40
.4	3.99	9.67	36.40	8.01
.5	5.71	11.62	36.97	10.21
.6	7.87	13.88	37.41	12.73
.7	10.68	16.55	37.71	15.73
.8	14.54	19.79	37.85	19.63
.9	20.95	23.55	37.86	25.47
1	∞	25.75	37.65	32.42
1.2	17.73	20.57	37.29	21.10
1.4	13.17	16.33	36.64	15.93
1.7	9.33	12.53	35.53	11.92
2	5.32	10.15	34.44	9.55
3	3.04	6.00	31.31	5.48
4	1.52	4.00	28.93	3.58
6	0.79	2.12	25.49	1.96
8	0.53	1.30	22.93	1.12
10	0.40	0.90	20.21	0.75
50	0.20	0.04	8.04	0.07
100	0.19	0.04	4.11	0.04

TABLE 9

Symmetrical Sideband Transmission Designs

Design Values } 60-Cycle Carrier Frequency, 10-Cycle Modulation Frequency

a	20	15	10
l	0.1763	0.32125	0.9776
m	1	1	1
g	0	0	0
ω/ω_o	Attenuation in Decibels		
.01	21.08	16.25	8.73
.05	21.11	16.29	8.79
.1	21.23	16.43	8.97
.2	21.70	16.94	9.66
.4	23.56	18.95	12.30
.5	25.98	20.44	13.83
.6	26.83	22.31	15.82
.7	29.19	24.66	18.13
.75	30.62	26.04	19.40
.8	32.36	27.62	20.72
.83333	33.62	28.77	21.61
.9	36.61	31.15	23.21
.91667	37.33	31.73	23.52
1	39.72	33.16	25.27
1.08333	37.15	31.59	23.39
1.16667	33.60	28.77	21.74
1.2	32.41	27.76	21.04
1.25	30.85	26.42	20.02
1.4	27.34	23.17	17.41
1.7	23.02	19.06	13.82
2	20.27	16.43	11.47
3	15.09	11.48	7.10
4	12.16	8.74	4.92
6	8.60	5.58	2.71
8	6.44	3.88	1.69
10	4.98	2.89	1.14
50	.32	.14	.05
100	.06	.02	.02

PRNC-3936-12-17-47-350